The latest updates of Polar Multi-sensor Aerosol product (PMAp)

Soheila Jafariserajehlou[1,2], Bertrand Fougnie[1], Andriy Holdak[1,3] , Margarita Vazquez-Navarro[1] , Alessandra Cacciari[1]

1 **EUMETSAT,** EUMETSAT-Allee 1, 64295 Darmstadt, Germany
2 **Rhea System GmbH**
3 **VisionSpace Technologies GmbH**

21th AeroCom / 10th AeroSAT meeting
Oslo, Norway, 10-14 October 2022

PMAP

Polar Multi-sensor Aerosol product (PMAp)

Metop
from **EUMETSAT** Polar System **(EPS)**

Near Real Time

Aerosol Optical Depth

and

Aerosol Type

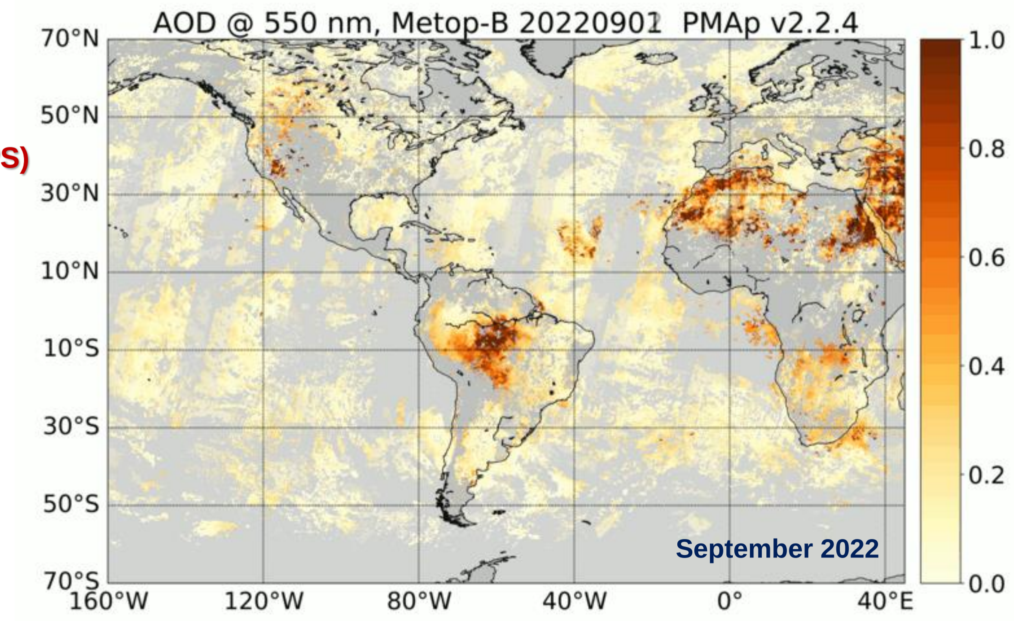
AOD @ 550 nm, Metop-B 20220901 PMAp v2.2.4

September 2022

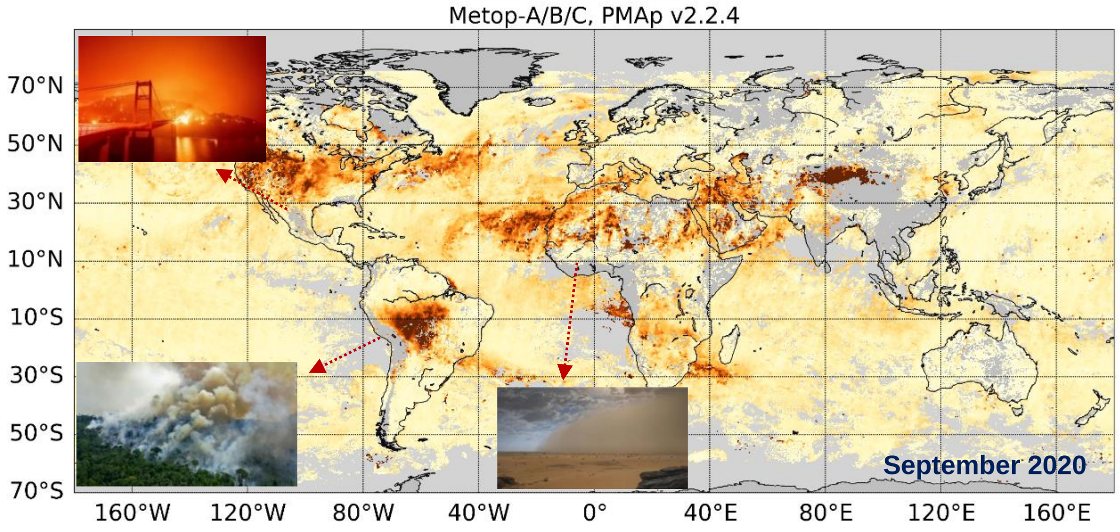
Metop-A/B/C, PMAp v2.2.4

September 2020

PMAp v2.2, daily AOD, Metop (A+B+C)

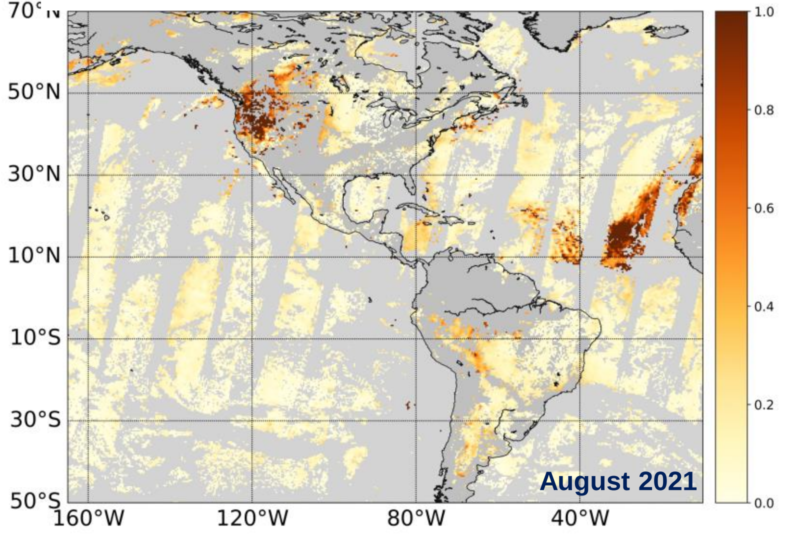
August 2021

PMAp v2.2, daily aerosol type, Metop (A+B+C)

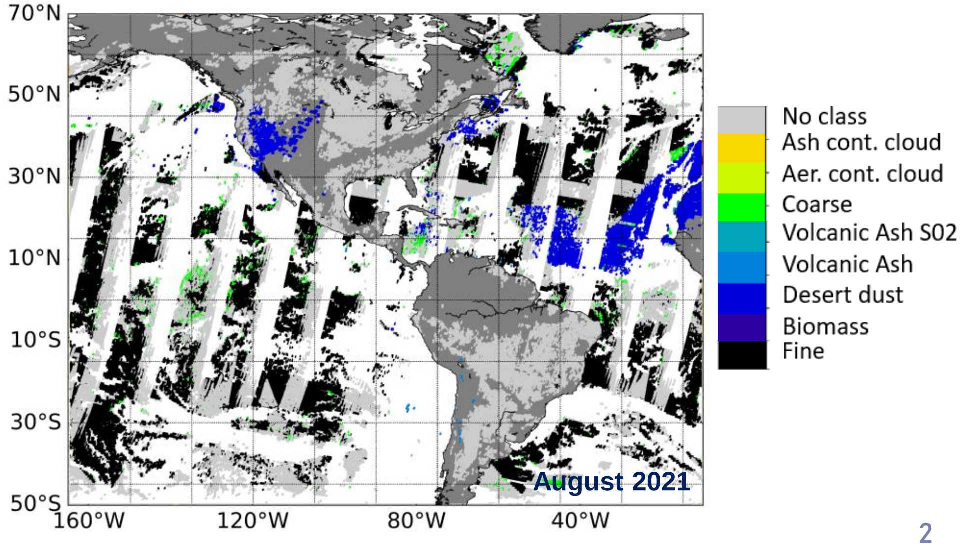
August 2021

PMAp: Synergy concept

- PMAp is an operational **synergistic** aerosol product retrieved from sensors on-board **Metop: AVHRR**, **IASI** and **GOME-2**;
- Dissemination started over ocean since April 2014;
- Over land since April 2016;
- Latest version: May 2021, coming revision: November 2022.

Metop

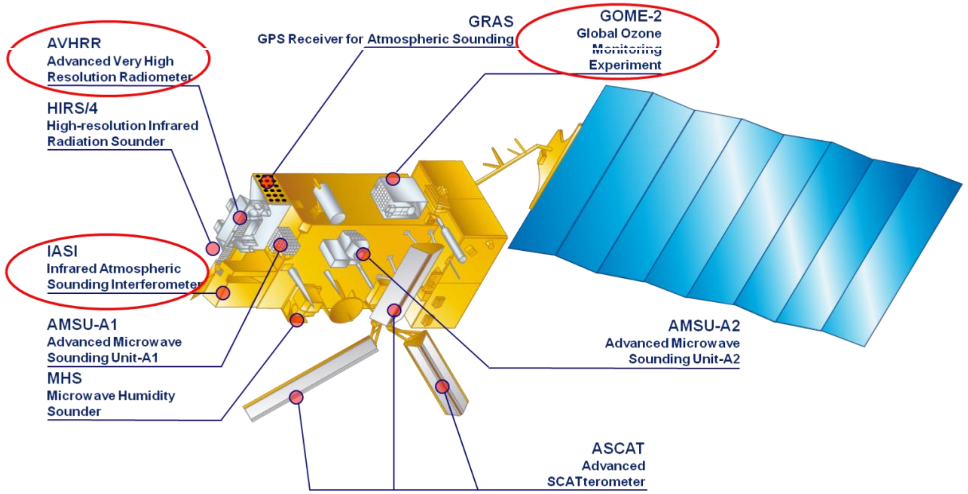

Multi-sensor spectral information

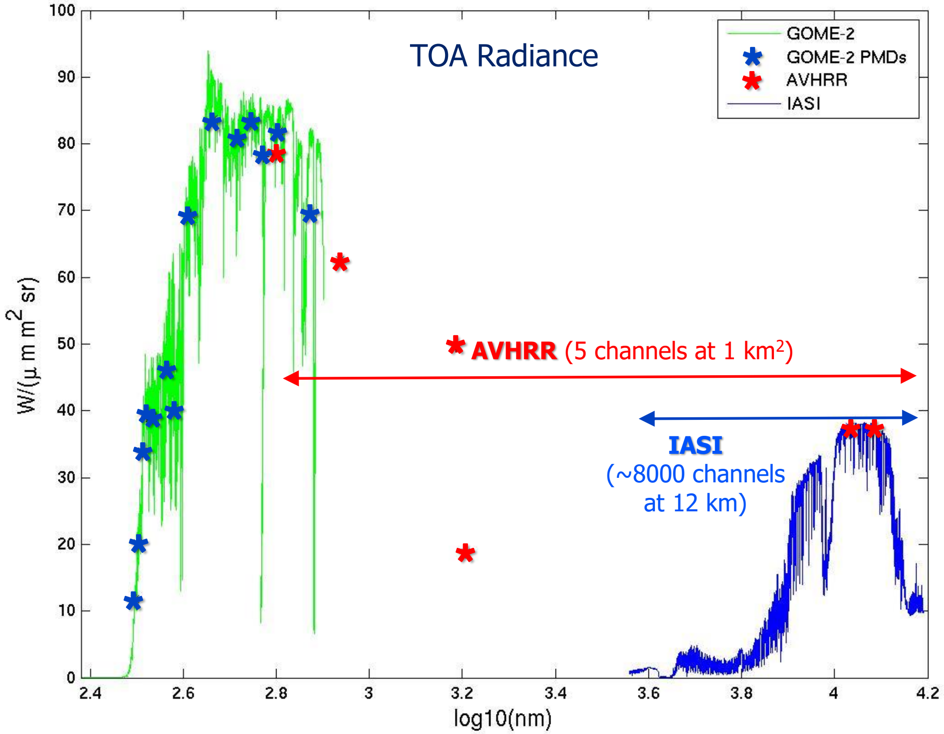

Multi-sensor co-location

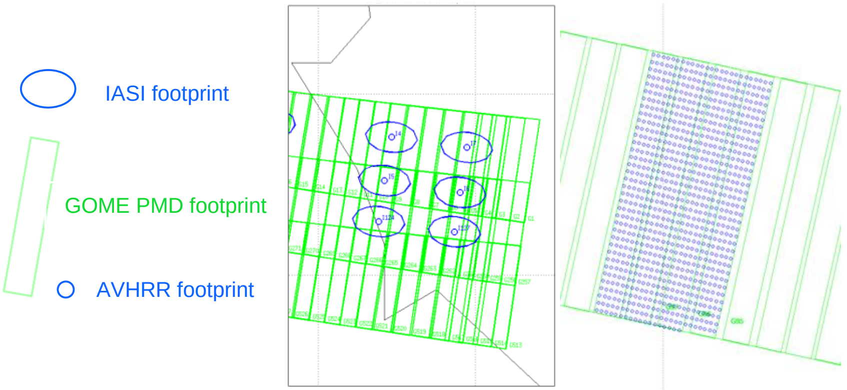

Merging hyper-spectral and high spatial information from GOME-2, AVHRR and IASI

Instruments	Spatial resolution	Spectral range	Polarisation
GOME-2 PMD	10×40 km^2	311 nm – 803 nm (15 bands)	Q/I
AVHRR	1.08 × 1.08 km^2	580 nm – 12500 nm (5 bands)	-
IASI	12 km (circular)	3700 nm – 15500 nm (resolution 0.5 cm^{-1})	-

Last release: PMAp v2.2

- ☐ **The current operational version:** v2.2.4 since 6th May 2021
  - A **dust** detection scheme exploiting IASI measurements;
  - Solving **hotspot issue**
  - Update and implementation of **Surface reflectance database** (LER);
  - **Radiometric correction**
  - Minimizing the **differences between AOD retrieved from Metop-A and B and C**.

- ☐ **Improvement of the consistency between Metop-A, B, and C over ocean.**
- ☐ **Significant improvement of the retrieval over Land.**

PMAp V2.1 Land

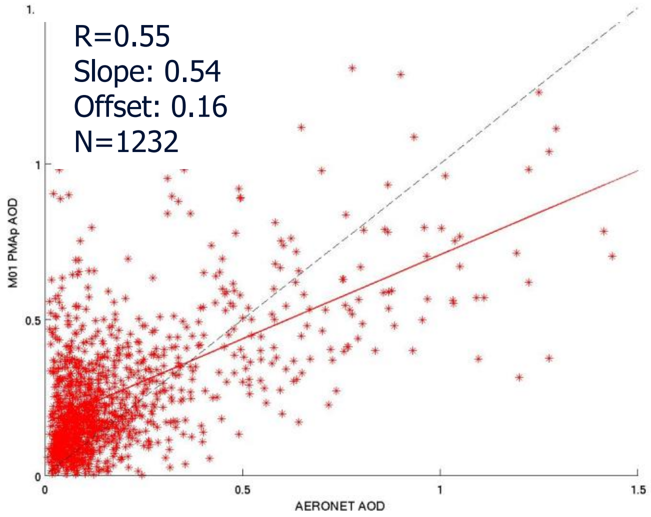

PMAp V2.2 Land

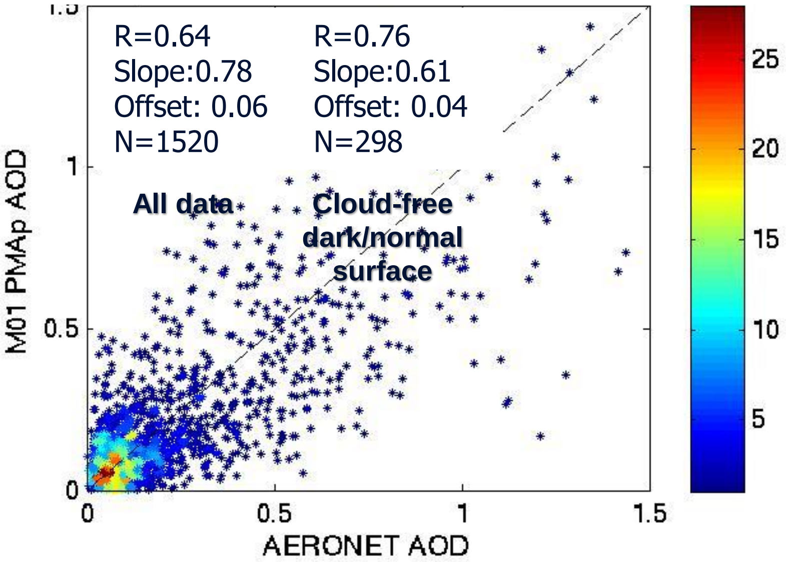

PMAp and MODIS/Terra, August 2021

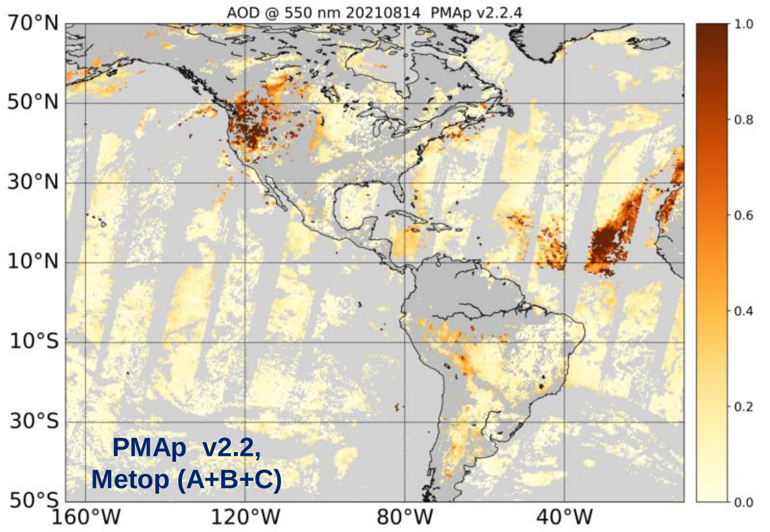

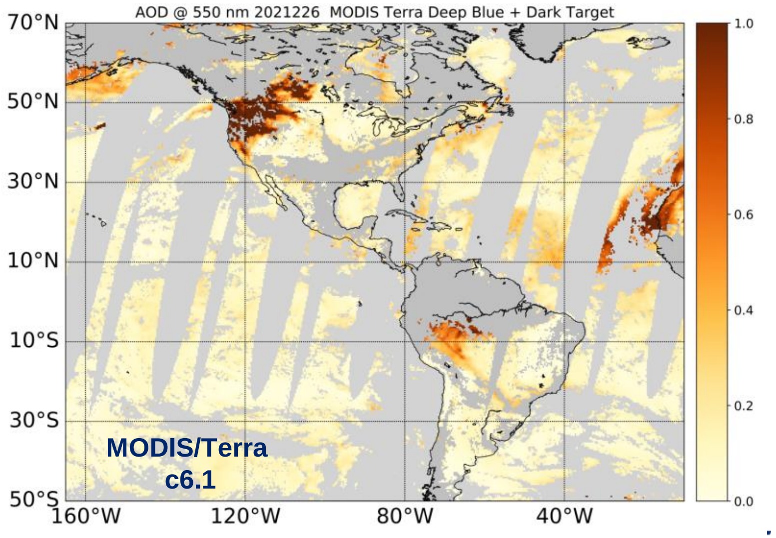

Limitations

Limitations of PMAp v2.2.4:

1) A cross track variation of AOD in PMAp retrieved by Metop-C;
2) Notable number of pixels with AOD = 0;
3) Differences between PMAp –B and –C;
4) Overestimation over bright land;
5) Anomalies due to surface reflectance database: GLER.

PMAp_AOD - MODIS_AOD 202108

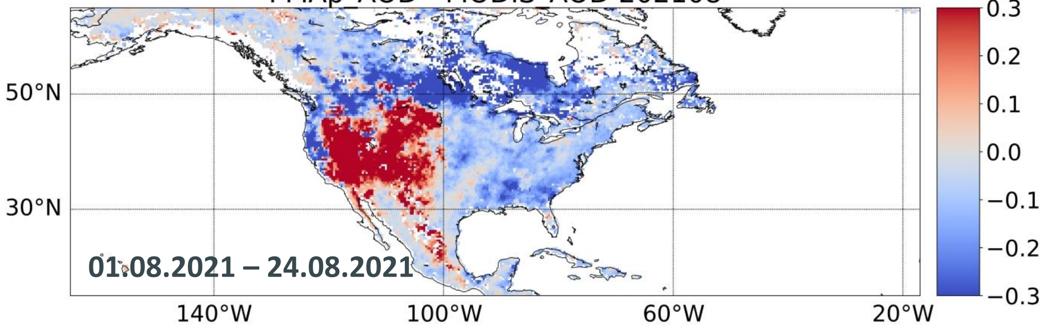

01.08.2021 – 24.08.2021

MODIS_surf_Ref - GOME2_minLER

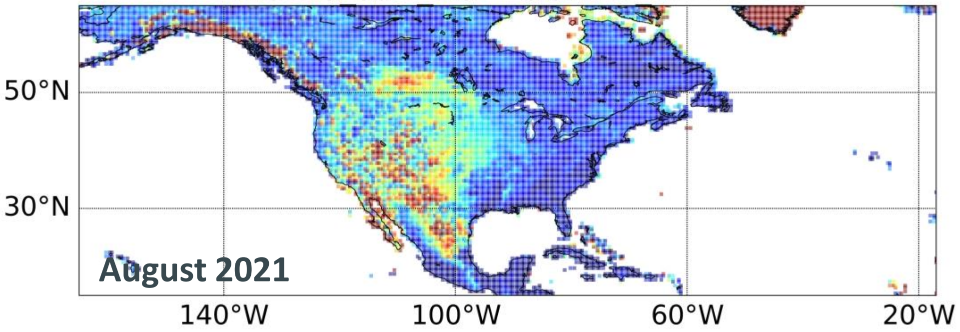

August 2021

AOD @ 550 nm, Metop-C 202209 PMAp v2.2.4

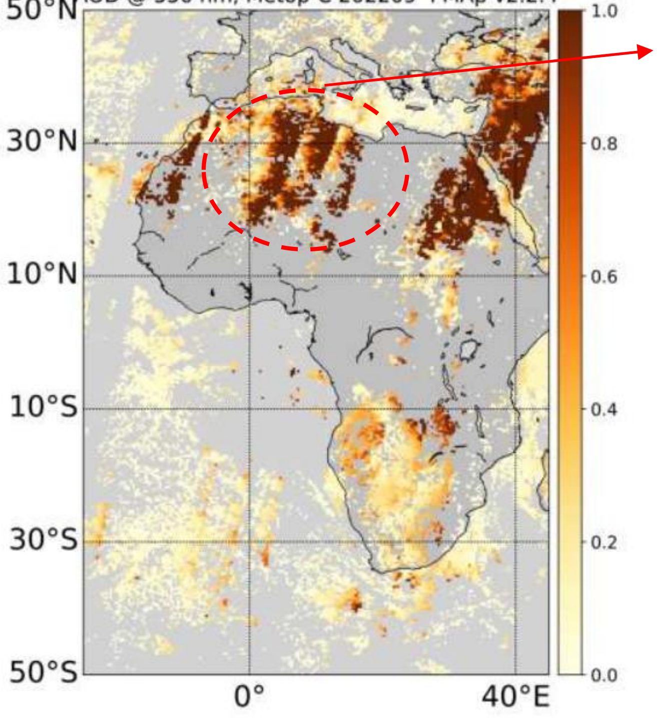

Artefacts in average AOD maps of Metop-C

Difference between PMAp-B & C

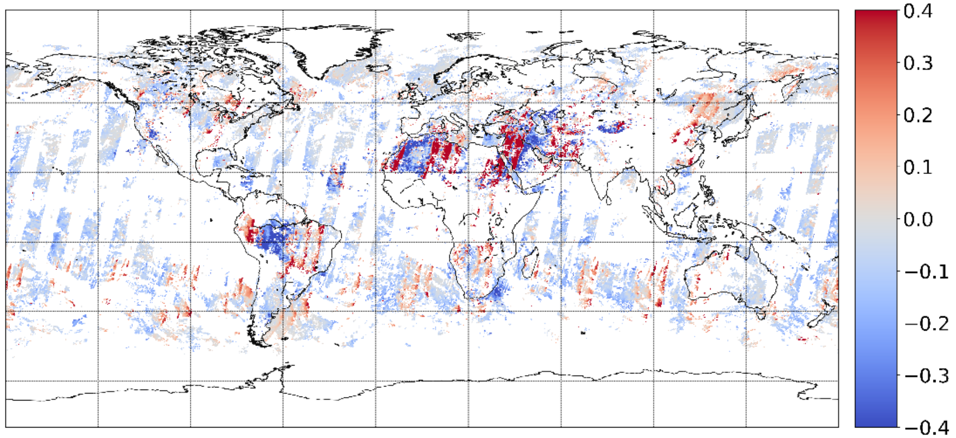

Difference between PMAp-B & C

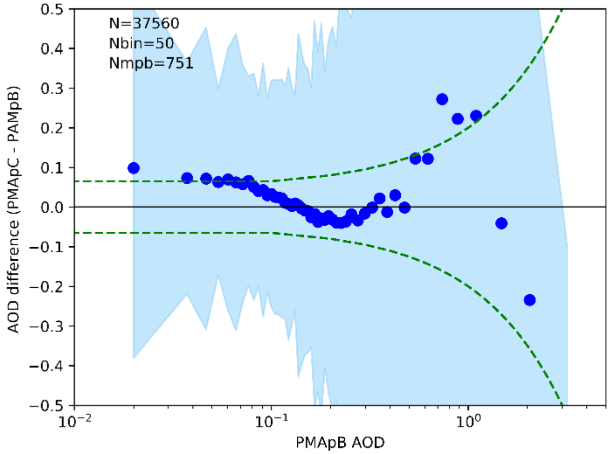

PMAp 2.2.5

t.int

To address the known limitations of PMAp 2.2.4:

1) Update of degradation correction to account for the aging of GOME-2 sensor;
1) Calculation of Radiometric adjustment for Metop-C;
2) Update of the radiometric adjustment for Metop-B;
3) Use of Mode-LER instead of Min-LER (ongoing analysis).

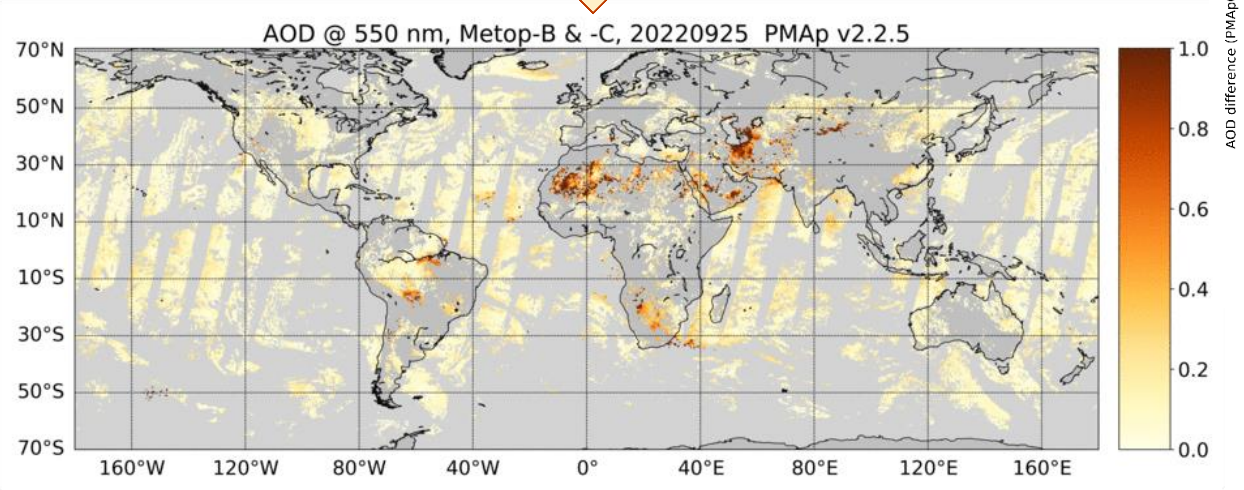

- Increasing the consistency between PMAp-B & -C
- Overall performance of PMAp-C improved.

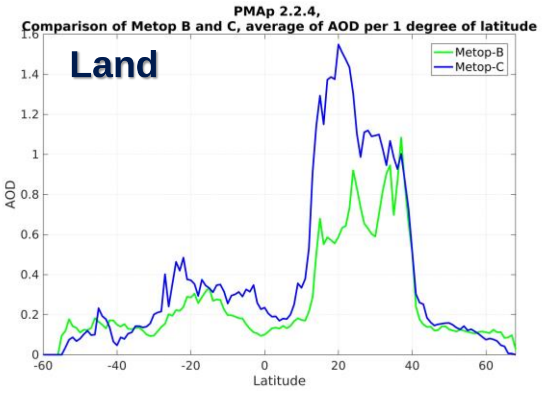

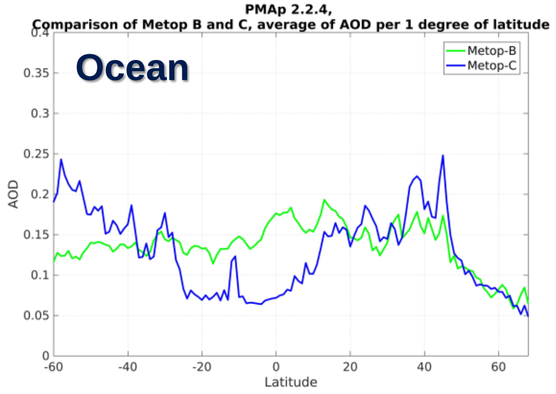

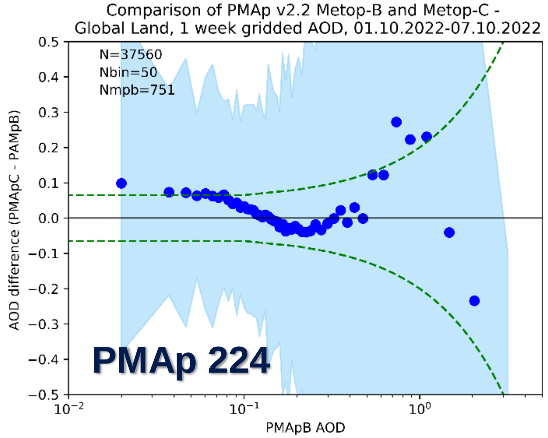

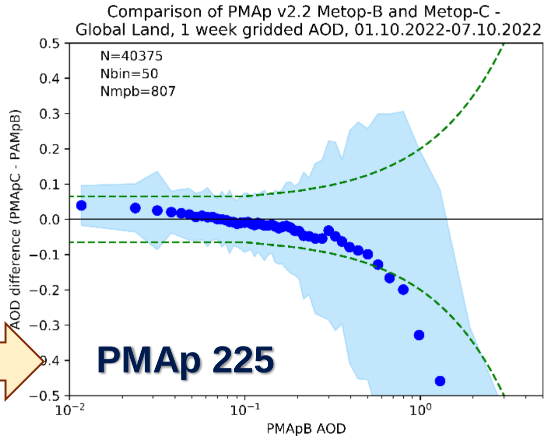

Validation vs AERONET

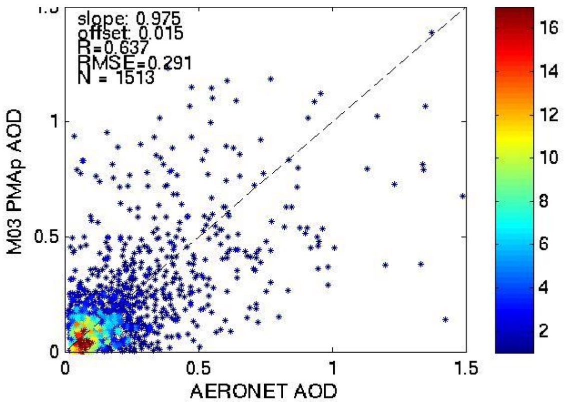

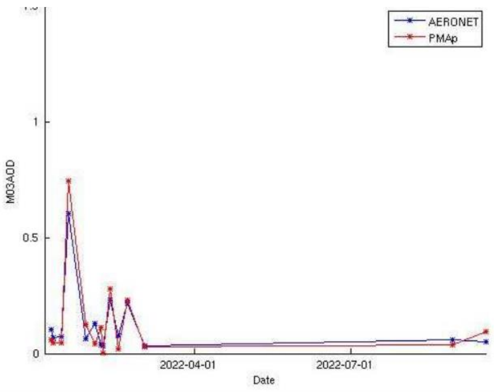

Summary

- PMAp v2.2 is operational since 6th May 2021:

  https://www.eumetsat.int/new-version-metop-pmap-product-released-soon

- PMAp v2.2 shows significant improvements compared to the previous operational version in terms of aerosol loading, spatial and temporal distribution, especially over land.
- The known limitations of PMAp 2.2.4 will be addressed in PMAp 2.2.5.
- Improvements compared to previous version, are indicated by internal validation.
- High consistency between the two Metops (-B & -C) is achieved, important for climate data records and time-series analysis

❖ **PMAp CDR (2007-2019)** is released! **See B. Fougnie talk, O11, Friday, 14 October.**

❖ **PMAp paper** is available for users: Grzegorski et al., Multi-sensor Retrieval of Aerosol Optical Properties for Near-Real-Time Applications Using the Metop Series of Satellites: Concept, Detailed Description and First Validation, Remote Sensing, 2022.

❖ **Europe operational NRT aerosol products** are expanding:

1) PMAp since 2014, new release in November 2022;
2) OSSAR CS-3 since 2020, new release soon! See J. Chimot talk, S4, Thursday 13 October;
3) 3MI, MAP synergy from EPS-SG, MAP/CO2M, MTG-FCI, future.

Assimilation of VIIRS Aerosol Optical Depth (AOD) within the Copernicus Atmosphere Monitoring Service (CAMS) data assimilation (DA) system

Sebastien Garrigues[1], Melanie Ades[1] , Samuel Remy[2], Julien Chimot[4], Johannes Flemming[1], Mark Parrington[1], Antje Inness[1], Zak Kipling[1], Roberto Ribas[1], Heather Lawrence[3], Richard Engelen[1] , Vincent-Henri Peuch[1]

1: ECMWF, Reading, UK
2: HYGEOS, France
3: MetOffice, Exeter, UK
4: EUMETSAT

Atmosphere Monitoring

CAMS GLOBAL AEROSOL DATA ASSIMILATION

Atmosphere Monitoring

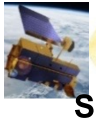

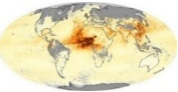

Satellite AOD

MODIS (AQUA, TERRA)
PMAp (METOP A,B,C)

Produce best optimal initial conditions

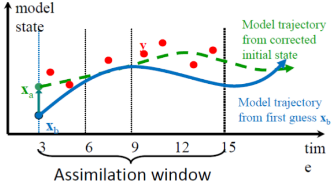

4D VAR data assimilation

Emission sources:
- satellite-based biomass burning (GFAS)
- emission inventories (anthropogenic, biogenic)

Integrated Forecasting Sytem (IFS)

- **Atmos. model**
  - Semi-Lagrangian advection model
  - 137 atm levels, ~40 km horizontal resolution
- **CB05 chemistry model** (Flemming et al., 2015; Huijnen et al, 2019)
- **Aerosol model** (Remy et al., 2019,2022):
  - Bulk-bin scheme
  - Species: sea salt, dust, organic matter, black carbon, sulfate, nitrate, amomium

- 5 day forecast,
- CAMS reanalysis

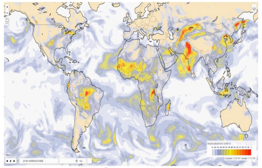

AOD, PM2.5, PM10

Experiment design

- ✓ **AOD retrieval assimilated in CAMS:**
  - ✓ Used in **operational forecast**:
    - MODIS (TERRA, AQUA; C6.1, DT+DB)
    - PMAp (Metop-A,B; v2.1; ocean only)
  - ✓ **Tested product**: VIIRS
    - NOAA EPS product
    - S-NPP, NOAA20
    - 0.750 km spatial resolution=>superobbing at ~40 km resolution
    - v2r1
- ✓ **Simulation period**: 02 June 2020- 30 November 2020 (evaluation on JJA and SON periods)

- ✓ **Experiments: impact of assimilating VIIRS**
  - **MODIS+PMAp versus MODIS+PMAp+VIIRS**
  - **MODIS only versus VIIRS only**

Atmosphere
Monitoring

First guess departure (satellite-model)

VIIRS

MODIS

Temporal average
June-August 2020

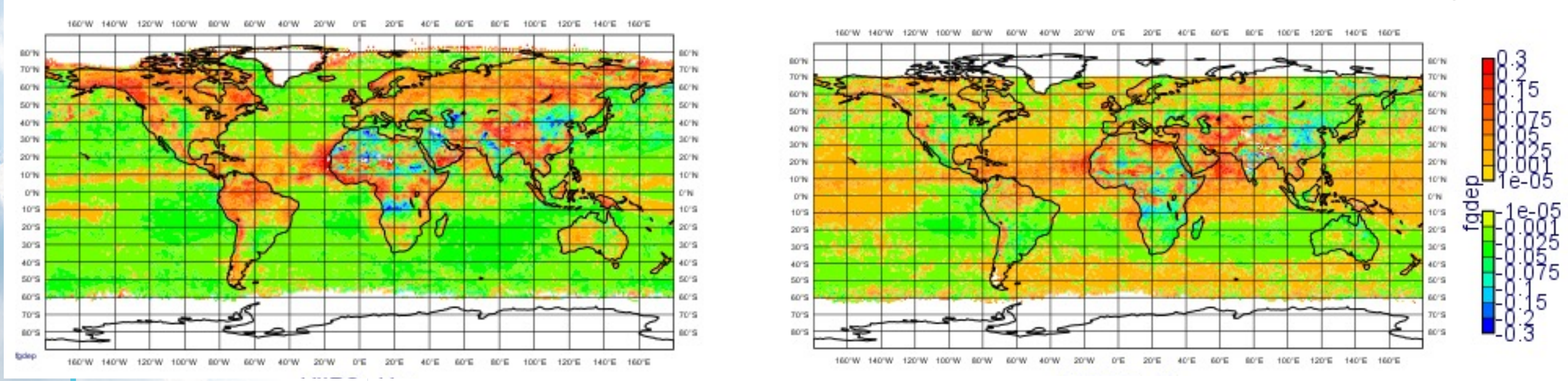

Ocean: VIIRS <model, MODIS > Model

Temporal average
June-August 2020

Land: VIIRS > model over dust source and biomass burning regions

European Commission | Copernicus Europe's eyes on Earth ECMWF

Results: Impact of assimilating VIIRS on analysis

Land

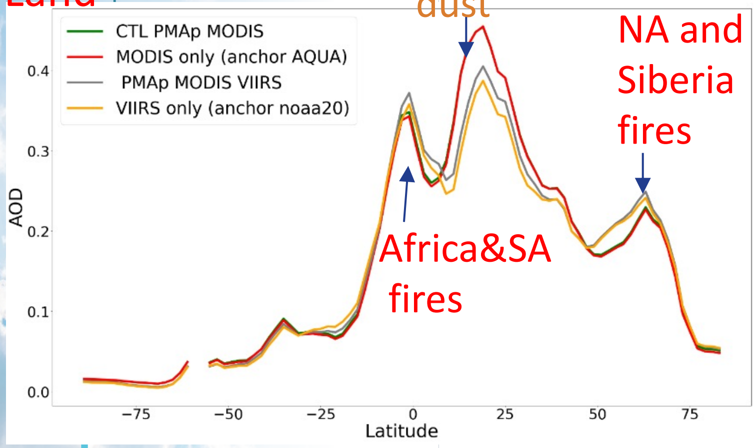

dust

NA and Siberia fires

Africa&SA fires

Ocean

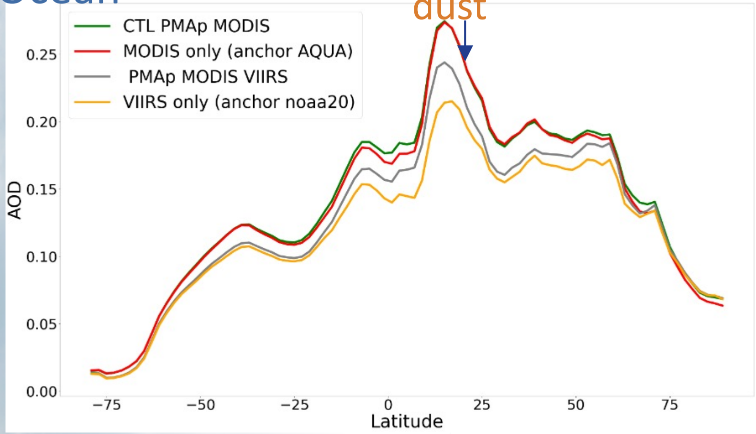

dust

VIIRS Only – MODIS Only analysis

AOD increases over biomass burning regions

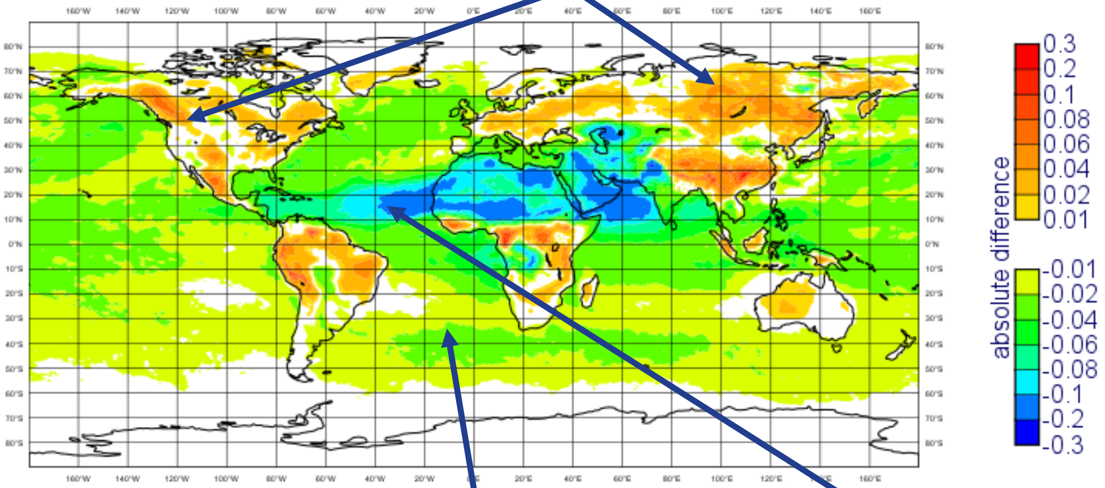

AOD decreases over ocean background and dust

Temporal average
June-August 2020

Global EVALUATION AGAINST AERONET

Atmosphere Monitoring

Global bias

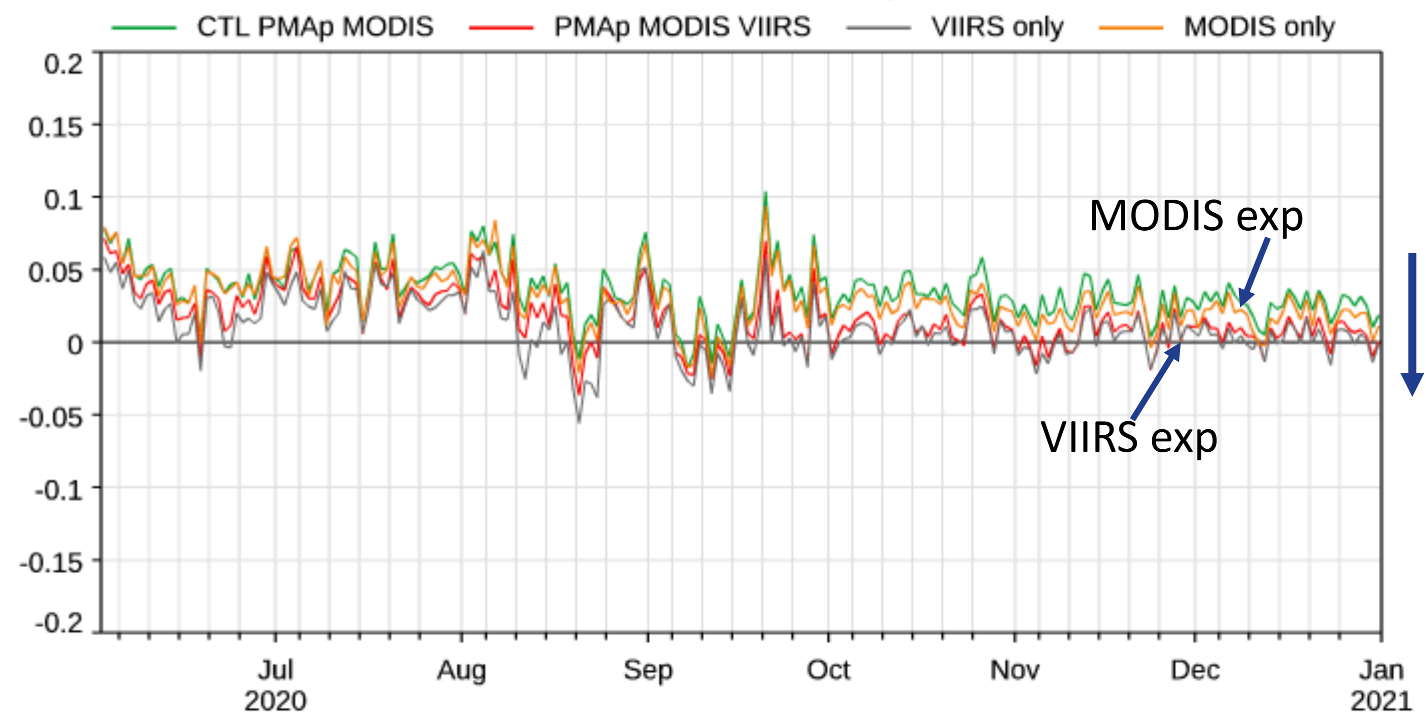

VIIRS assimilation

Bias reduction

EXP$_{CTL}$: MODIS, PMAp

EXP$_{PMV}$: MODIS, PMAp, VIIRS

EXP$_{V}$: VIIRS only (anchor SNPP)

EXP$_{M}$: MODIS only (anchor AQUA)

European Commission | Copernicus Europe's eyes on Earth | ECMWF

Atmosphere Monitoring

Conclusions

✓ VIIRS versus MODIS AOD within CAMS

- Overall good consistency between VIIRS and MODIS
- VIIRS < MODIS over ocean background and dust outbreak in the Atlantic
- VIIRS>MODIS over biomass burning regions

✓ Impact of assimilating VIIRS

- **Lower increment over ocean** and mid-Atlantic dust outbreak
- **Higher increment over biomass burning regions**

✓ Impact on the forecast

- Positive impact on AOD forecast: reduction of bias, particularly for Europe and desert sites

European Commission | Copernicus Europe's eyes on Earth ECMWF

Atmosphere Monitoring

- ADDITIONAL SLIDES

SATELLITE AOD USED IN CAMS

Products used in operational assimilation

- **MODIS**
  - AQUA, TERRA
  - C6
  - DB+DT product
  - 10 km
  - Land and ocean
  - Thinning
  - Spatially constant obs error

- **PMAp**
  - METOP-A,B,C
  - From GOME-2+IASI+AVHRR
  - V2.1
  - 40*10 km
  - Assimilated over ocean only
  - Thinning
  - Pixel-level observation error +inflation

Monitored/tested new product

- **NOAA-EPS VIIRS**
  - NOAA-20 and S-NPP
  - V2r1
  - 0.750m
  - Land and ocean
  - Superobbing
  - Pixel-level observation error

Experiment design

Experiments	Model	MODIS	VIIRS	PMAp
PMAp, MODIS - 47r3	47r3	Anchor: TERRA and AQUA	No	Bias Corrected
PMAp, MODIS, VIIRS-47r3	47r3	Bias Corrected	Bias Correction : SNPP, Anchor: NOAA20	Bias Corrected
VIIRS only-47r3	47r3	NO	Bias Correction : SNPP, Anchor: NOAA20	No
MODIS Only-47r3	47r3	Bias Corrected : TERRA, Anchor: AQUA	No	No
PMAp, MODIS-48r1	48r1	Anchor: TERRA and AQUA	No	Bias Corrected
PMAp, MODIS, VIIRS – 48r1	48r1	BC	Bias Correction : SNPP, Anchor: NOAA20	Bias Corrected

Atmosphere
Monitoring

P M EVALUATION AGAINST AIRCHINA

PM2.5

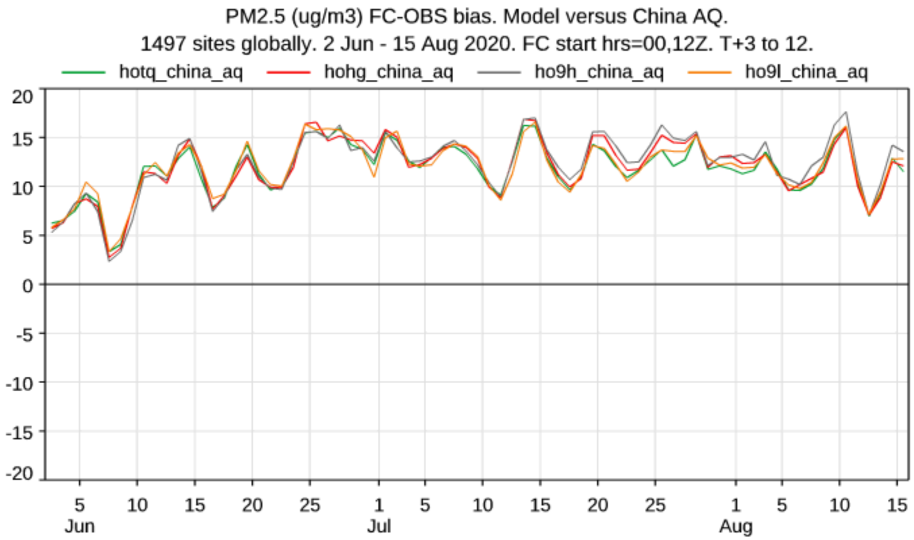
PM2.5 (ug/m3) FC-OBS bias. Model versus China AQ.
1497 sites globally. 2 Jun - 15 Aug 2020. FC start hrs=00,12Z. T+3 to 12.

PM10

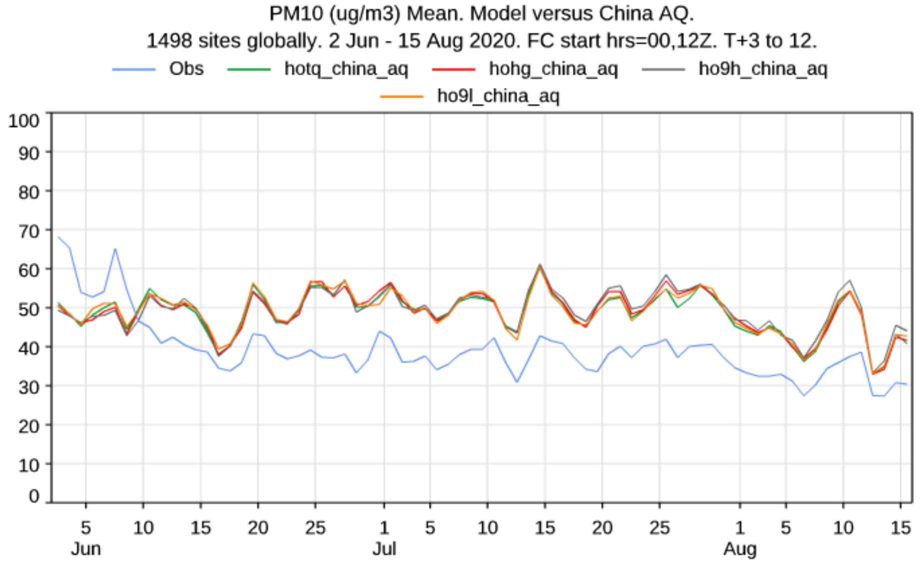
PM10 (ug/m3) Mean. Model versus China AQ.
1498 sites globally. 2 Jun - 15 Aug 2020. FC start hrs=00,12Z. T+3 to 12.

No significant differences between experiments
No significant impact of VIIRS assimilation

- EXP_{CTL} : MODIS, PMAp
- EXP_{PMV} : MODIS, PMAp, VIIRS
- EXP_{V} : VIIRS only (anchor SNPP)
- EXP_{M} : MODIS only (anchor AQUA)

Summer 2020 atmospheric composition events

Atmosphere Monitoring

SIBERIA FIRE

OM AOD (FC)

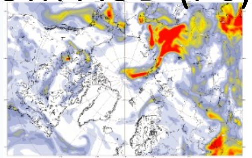

CALIFORNIA FIRES

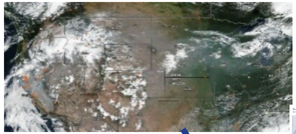

OM AOD (FC)

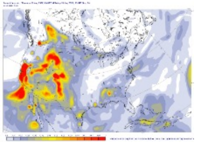

SOUTH AMERICA FIRES

OM (AN)

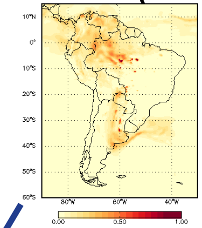

FRP

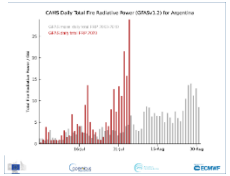

DUST (godzilla event)

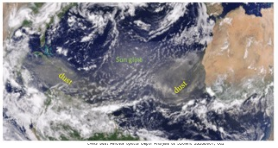

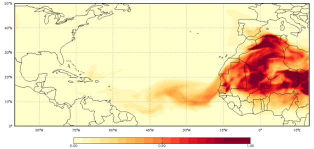

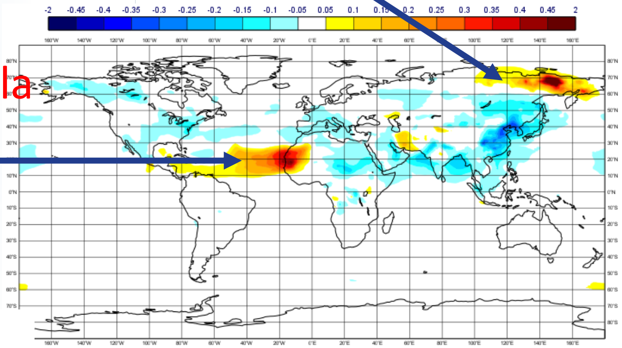

CAMS June AOD anomalies

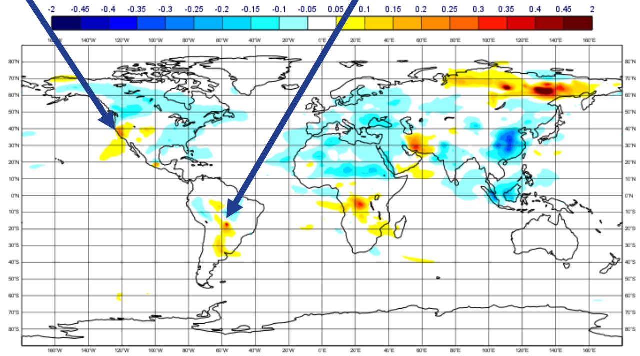

CAMS August AOD anomalies

European Commission | Copernicus Europe's eyes on Earth ECMWF

Credit: Mark Parrington (CAMS weather room, June-Sept 2020)

Impact of data assimilation(DA) on forecasts

CAMS AOD forecast bias against AERONET

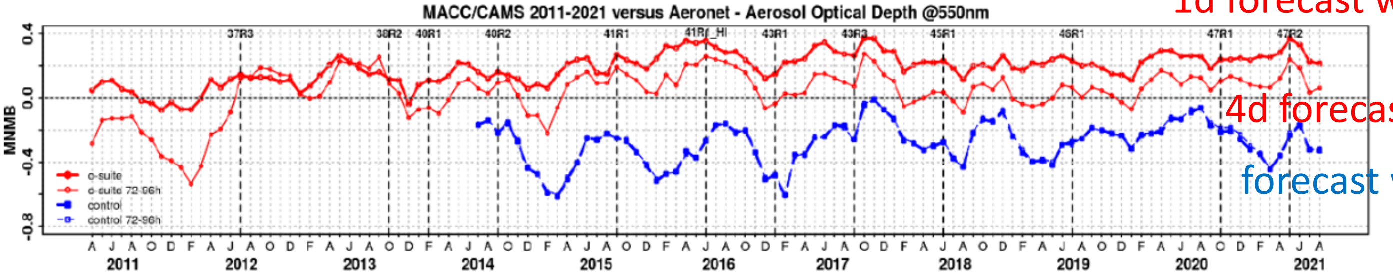

1d forecast with DA

4d forecast with DA

forecast without DA

Positive impact on AOD

AMS PM2.5 forecast compared to EMEP and IMPROVE ground observations

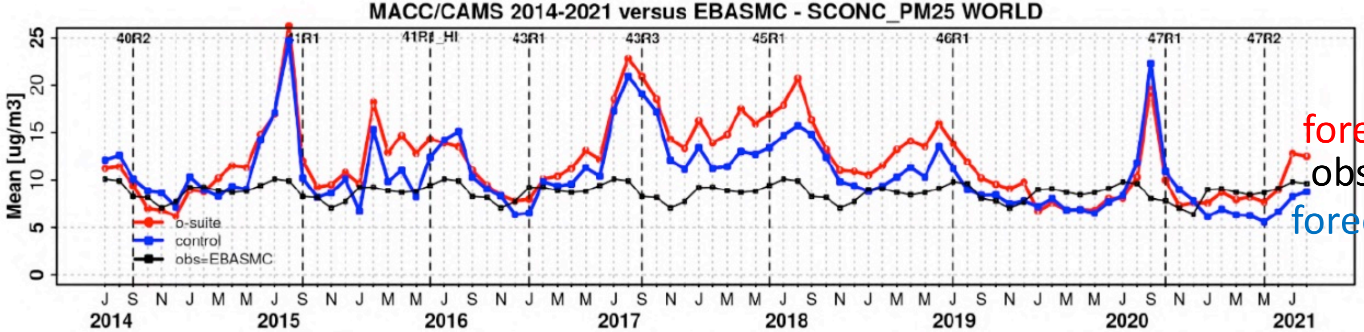

forecast with DA

observations

forecast without DA

Mixed result for PM2.5

Copernicus Europe's eyes on Earth

ECMWF

Credit: CAMS validation report (CAMS84_2018SC3_D1.1.1_JJA2021)

Comparison of VIIRS and MODIS AOD

Satellite AOD latitude transect (ocean and land)

Temporal average
June-August 2020

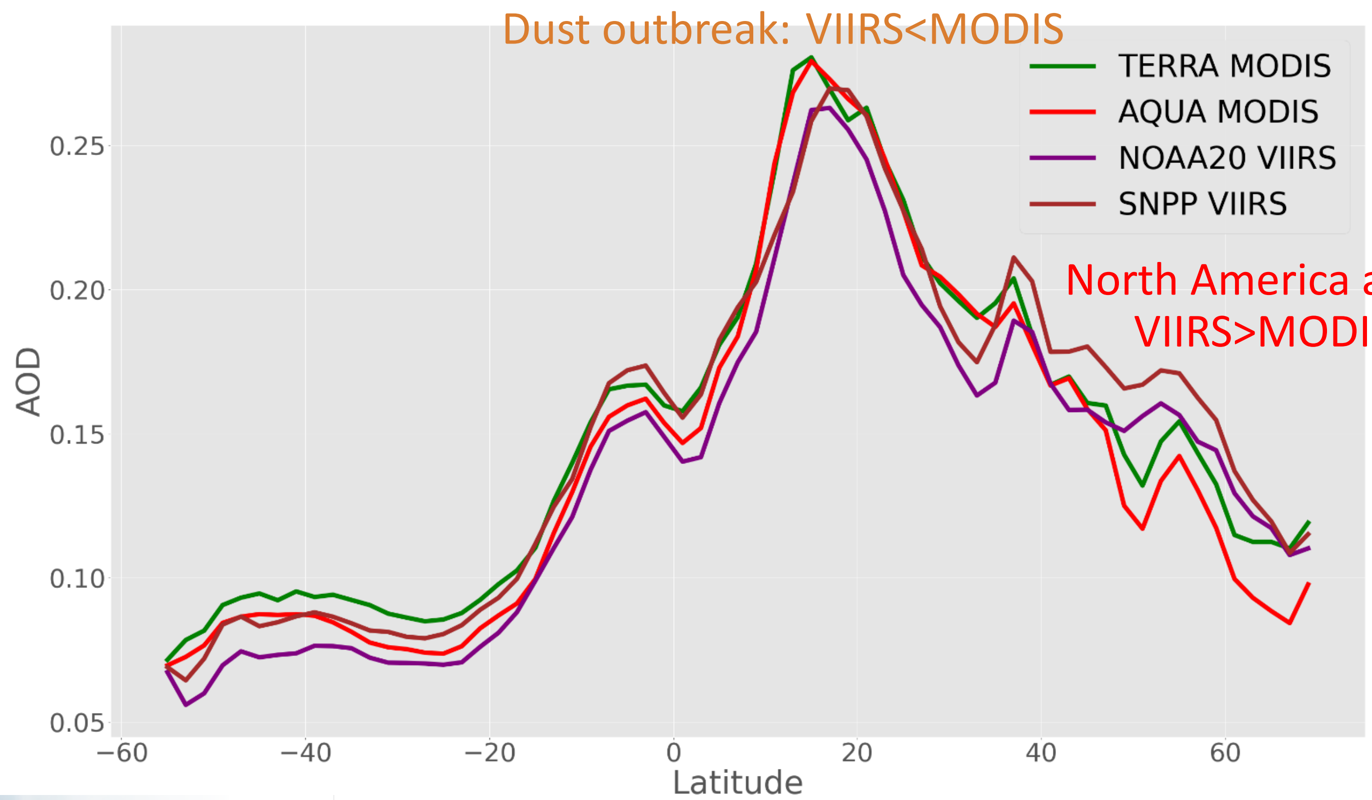

Dust outbreak: VIIRS<MODIS

North America and Siberia fires
VIIRS>MODIS

Atmosphere Monitoring

Impact of assimilation window

00z
3pm to 3am

12z
3am to 3pm

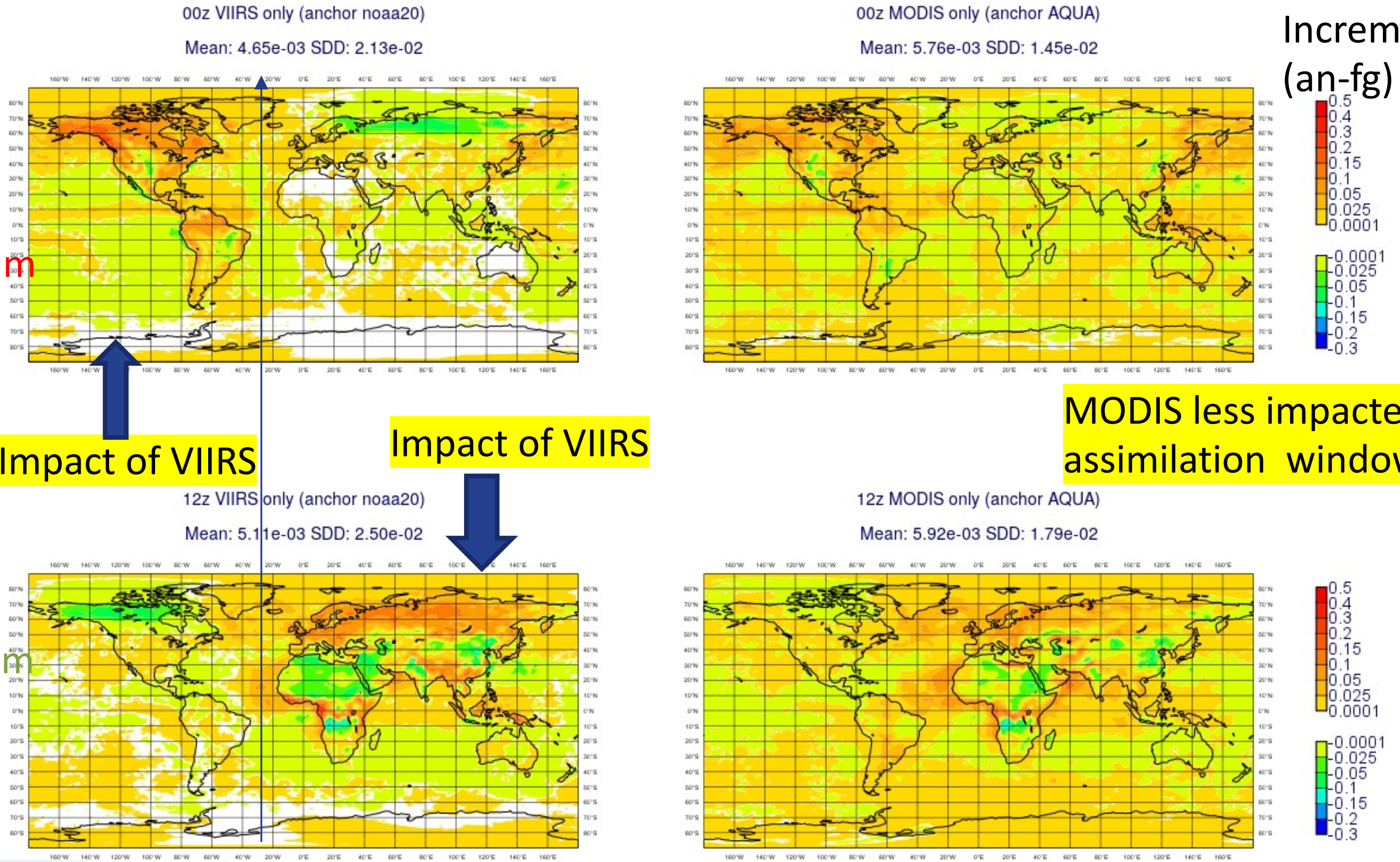

00z VIIRS only (anchor noaa20)
Mean: 4.65e-03 SDD: 2.13e-02

00z MODIS only (anchor AQUA)
Mean: 5.76e-03 SDD: 1.45e-02

12z VIIRS only (anchor noaa20)
Mean: 5.11e-03 SDD: 2.50e-02

12z MODIS only (anchor AQUA)
Mean: 5.92e-03 SDD: 1.79e-02

Increments (an-fg)

Impact of VIIRS

Impact of VIIRS

MODIS less impacted by assimilation window

Regional EVALUATION AGAINST AERONET

bias

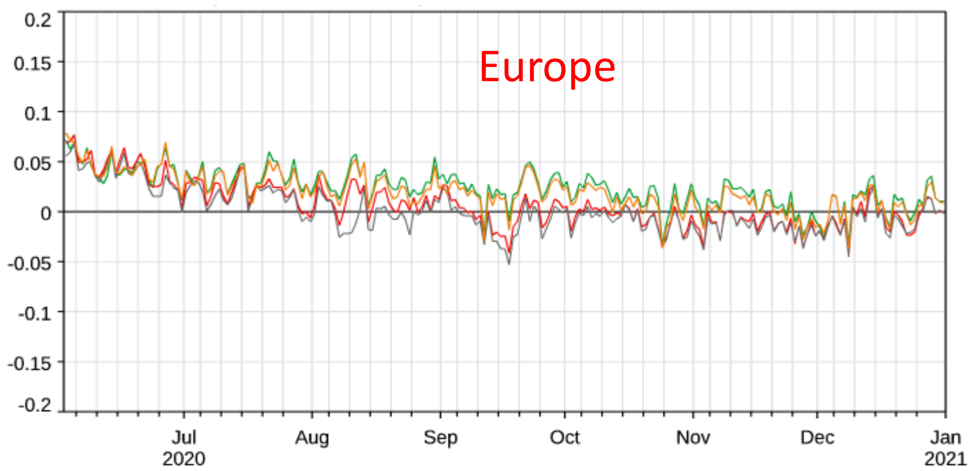
Europe

VIIRS assimilation

Bias reduction

bias

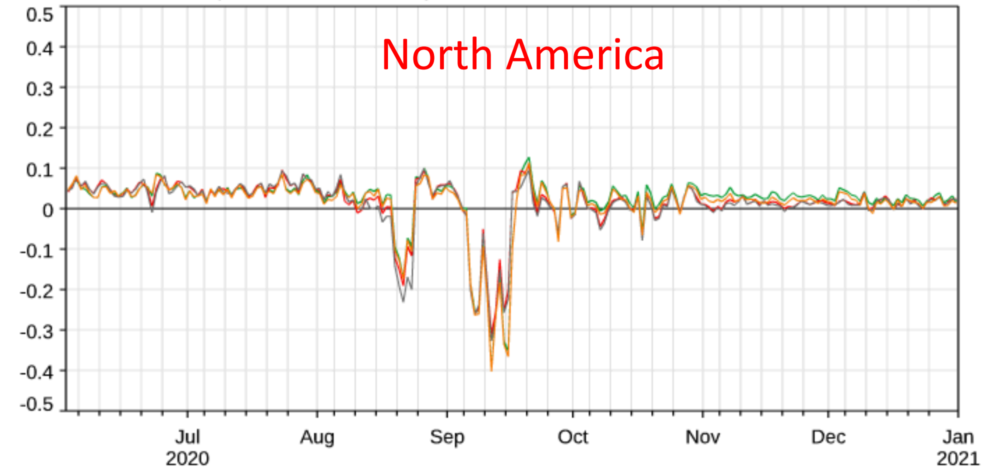
North America

VIIRS assimilation: No significant impact

- 🟩 EXP_{CTL} : MODIS, PMAp
- 🟥 EXP_{PMV} : MODIS, PMAp, VIIRS
- ▬ EXP_{V} : VIIRS only (anchor SNPP)
- 🟧 EXP_{M} : MODIS only (anchor AQUA)

Regional EVALUATION AGAINST AERONET

Desert sites

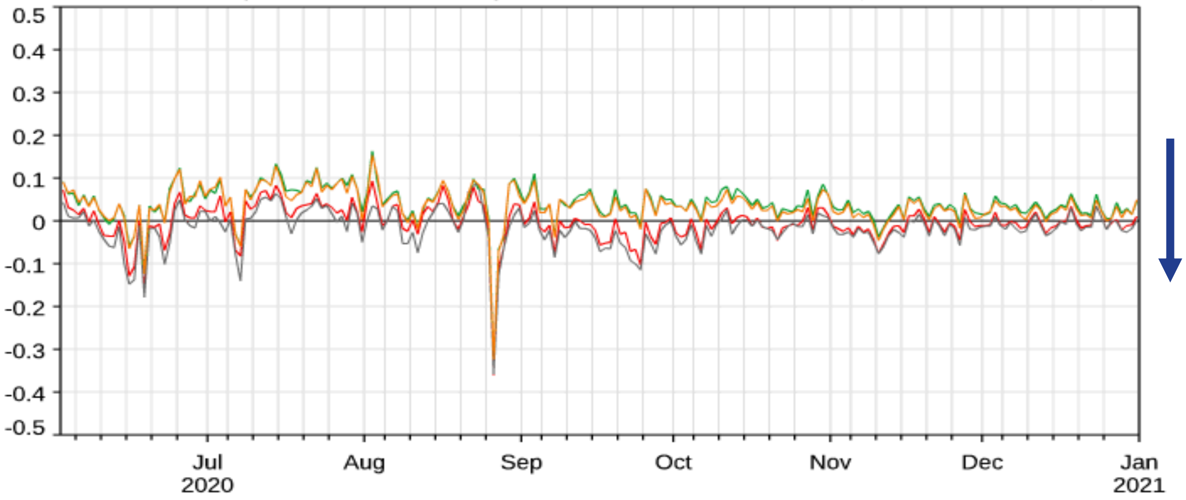

VIIRS assimilation

Bias reduction

Oceanic sites

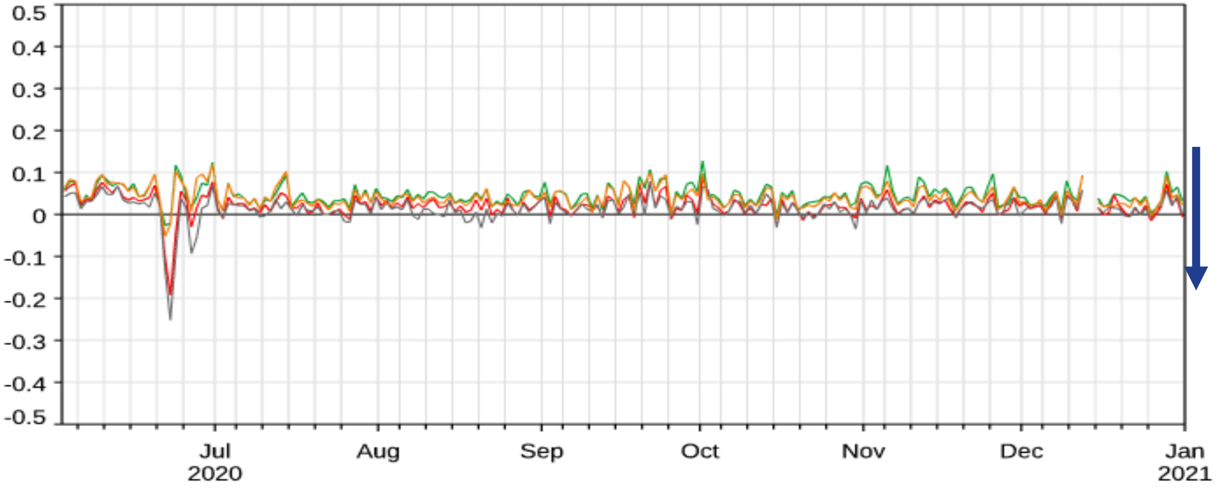

Slight bias reduction

- 🟩 EXP_{CTL} : MODIS, PMAp
- 🟥 EXP_{PMV} : MODIS, PMAp, VIIRS
- ⬛ EXP_{V} : VIIRS only (anchor SNP
- 🟧 EXP_{M} : MODIS only (anchor A

Atmosphere Monitoring

PM EVALUATION AGAINST AIRBASE(Europe)

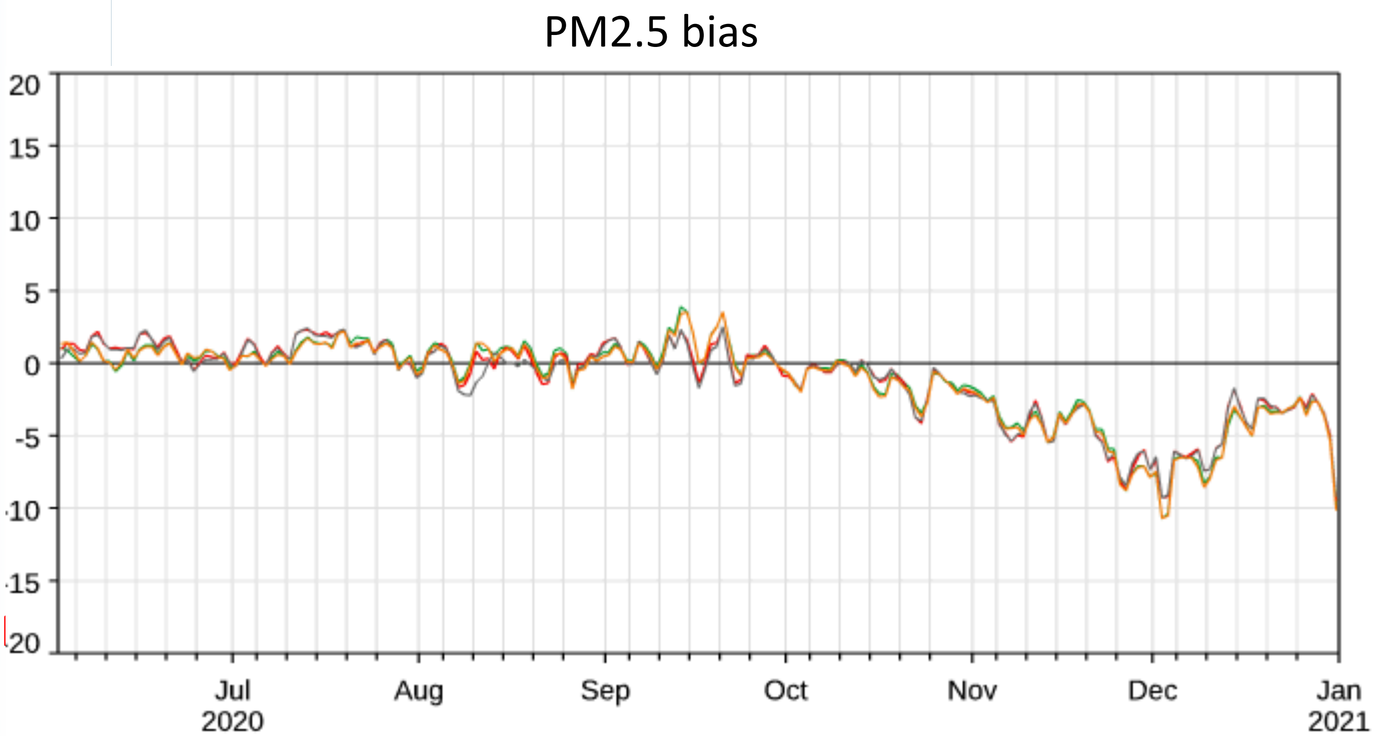

🟩 EXP_{CTL} : MODIS, PMAp

🟥 EXP_{PMV} : MODIS, PMAp, VIIRS

⬛ EXP_{V} : VIIRS only (anchor SNPP)

🟧 EXP_{M} : MODIS only (anchor AQUA)

Atmosphere Monitoring

PM2.5 EVALUATION AGAINST AIRNOW(US)

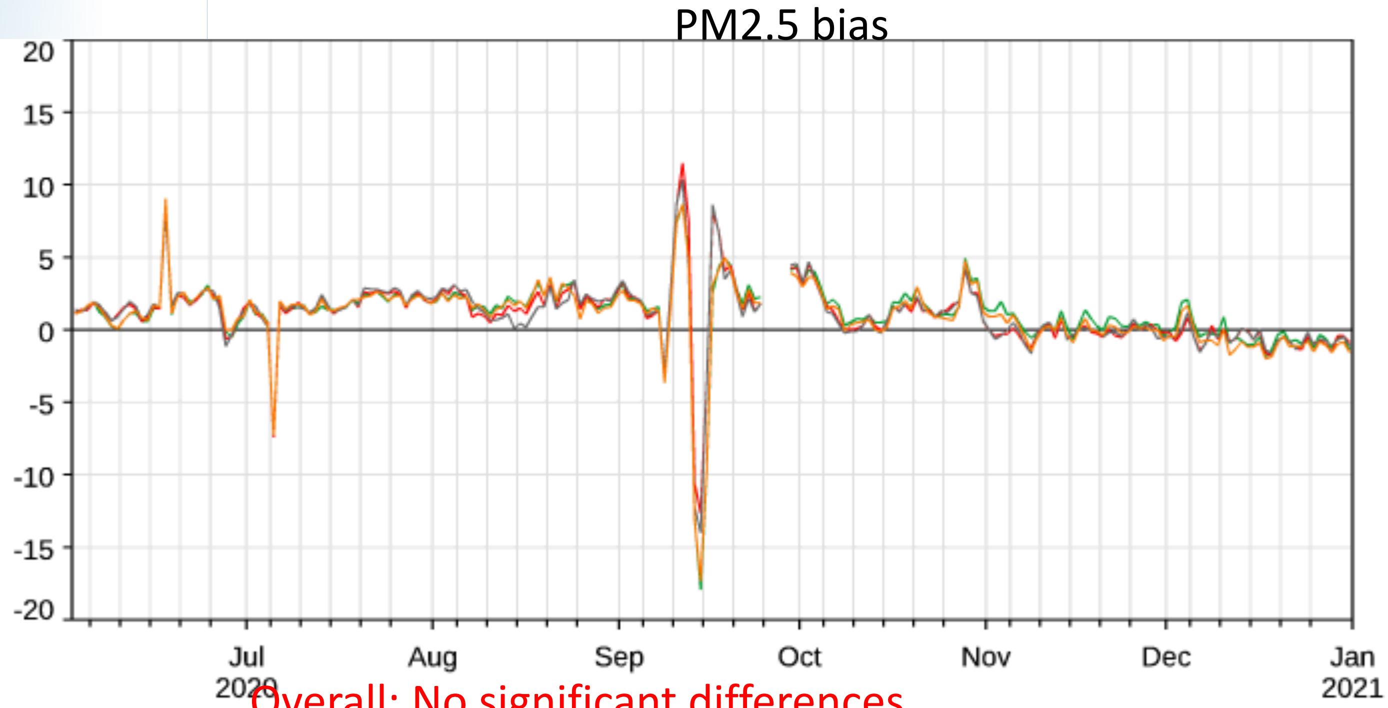

Overall: No significant differences

Mid-August: reduction of bias for the California fire season

🟩 EXP_{CTL} : MODIS, PMAp

🟥 EXP_{PMV} : MODIS, PMAp, VIIRS

⬛ EXP_{V} : VIIRS only (anchor SNPP)

🟧 EXP_{M} : MODIS only (anchor AQUA)

European Commission | Copernicus Europe's eyes on Earth ECMWF

Constraining aerosol properties using polarimetric satellite observations

Guangliang Fu, Cheng Chen, Pavel Litvinov, Oleg Dubovik, Sha Lu, Bastiaan van Diedenhoven, Otto Hasekamp (O.Hasekamp@sron.nl)

Netherlands Institute for Space Research

Netherlands Organisation for Scientific Research (NWO)

Multi-Angle Polarimetry: Comparing SRON-RemoTAP and GRASP

Expectations from multi-angle polarimetry:

- ✓ Improved accuracy on existing products (AOD)
- ✓ More information → new products such as size, absorption, composition/type, shape.
- ✓ Simultaneous retrieval of aerosol – surface – ocean – cloud properties

But very challenging to exploit this large information content at a global scale.

- ✓ Complex algorithms needed with many fit parameters (aerosol+surface/ocean).
- ✓ Accurate/detailed forward model with online RT calculations.
- ✓ Challenging instrumentation (multi-angle registrations, radiometric/polarimetric uncertainties

2 algorithms with global capability:

- ✓ SRON RemoTAP (*Hasekamp et al., 2011; 2019; Fu et al., AMT, 2018;2020*)
- ✓ GRASP (*Dubovik et al., 2011, 2014, 2021; Chen et al 2020*)

ESA HARPOL Project

- ✓ Comparing existing RemoTAP and GRASP data products
- ✓ Systematic comparison for synthetic retrievals
- ✓ Improving RemoTAP and GRASP algorithms
- ✓ Global processing for year 2008 with improved algorithms
- ✓ Comparing improved data products

Polarimeters in Space

2005 2013 2024 2025 2026

POLDER-3 / PARASOL

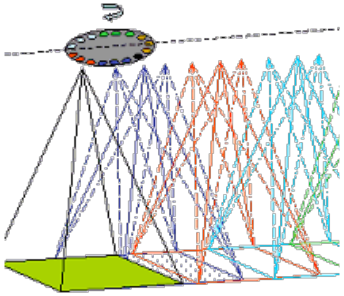

>10 year GAP!

PACE

SPEXone – PACE

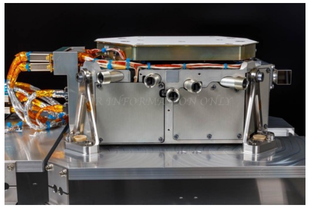

HARP2 – PACE

3MI

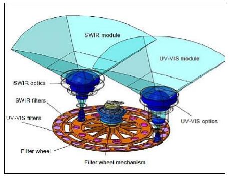

CO2M

MAP

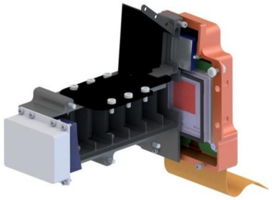

RemoTAP and GRASP PARASOL retrievals over Land

SRON-RemoTAP (3-mode)

AOD (amount)

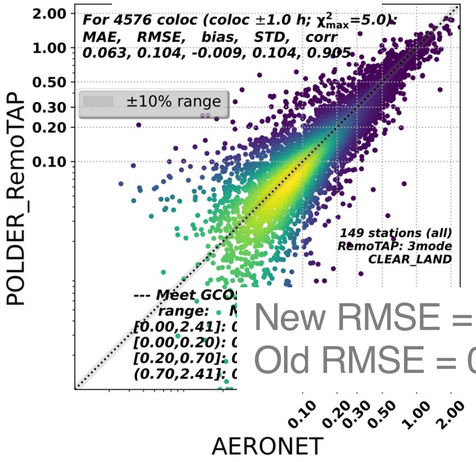

New RMSE = 0.10
Old RMSE = 0.18

AE (size)

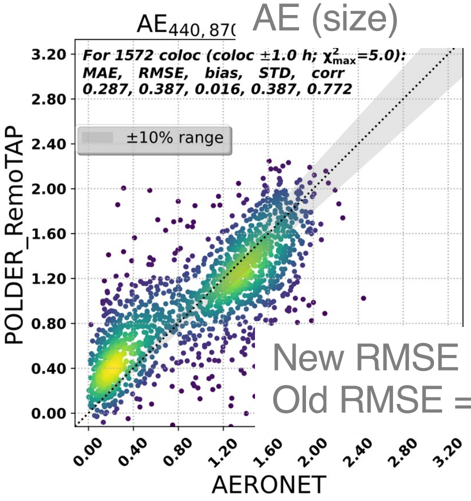

New RMSE = 0.39
Old RMSE = 0.63

SSA (absorption)

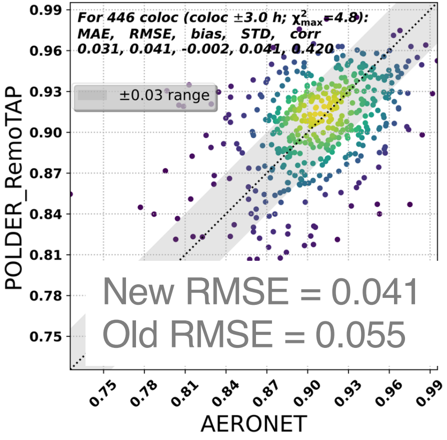

New RMSE = 0.041
Old RMSE = 0.055

GRASP (Component)

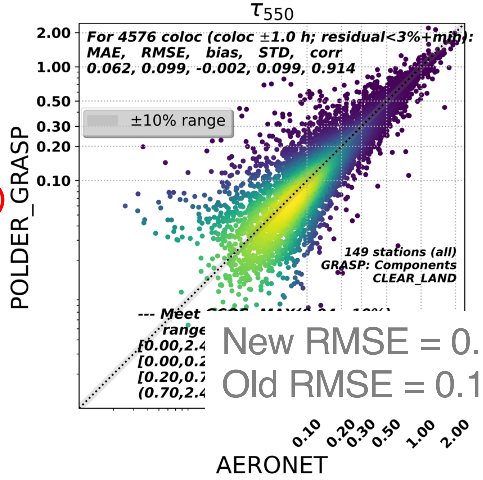

New RMSE = 0.10
Old RMSE = 0.16

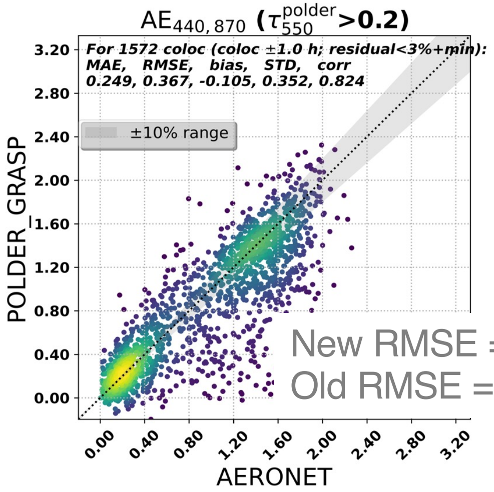

New RMSE = 0.37
Old RMSE = 0.38

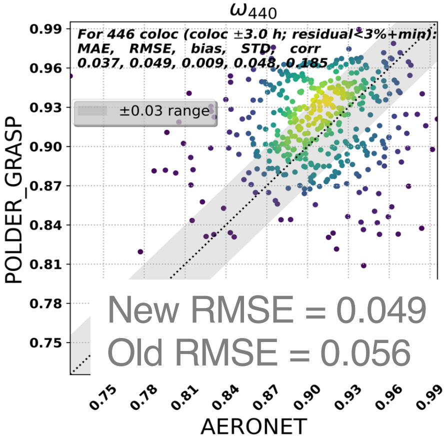

New RMSE = 0.049
Old RMSE = 0.056

Figures by Guangliang Fu

Comparison of Global PARASOL Products 2008 (Jan-Nov)

AOD (amount)　**AE (AOD > 0.2)**　**SSA (AOD > 0.3)**

GRASP

SRON-RTP

difference

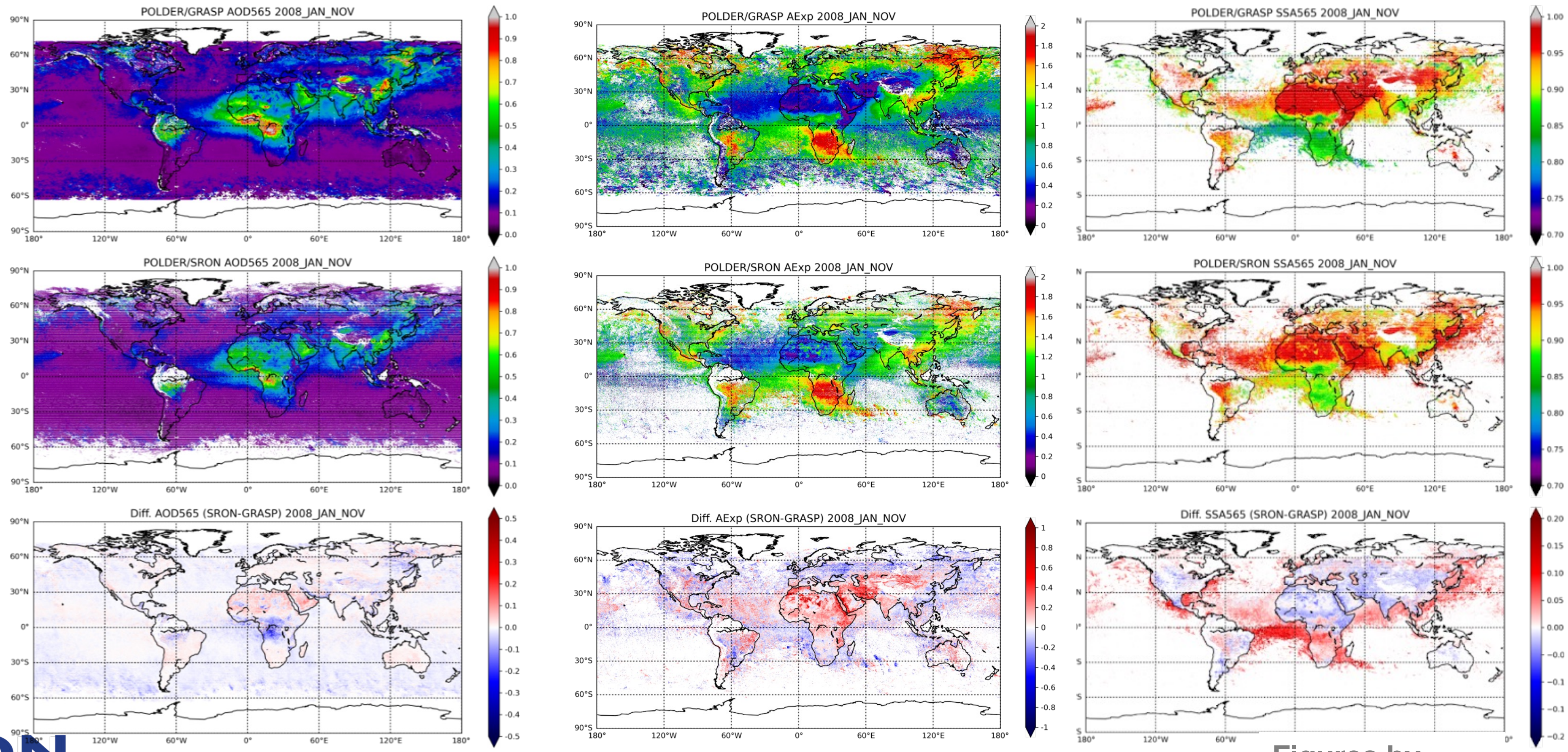

Figures by Cheng Chen

Comparison of Global PARASOL Products 2008 (Jan-Nov)

AOD

AE (AOD > 0.2)

SSA (AOD > 0.3)

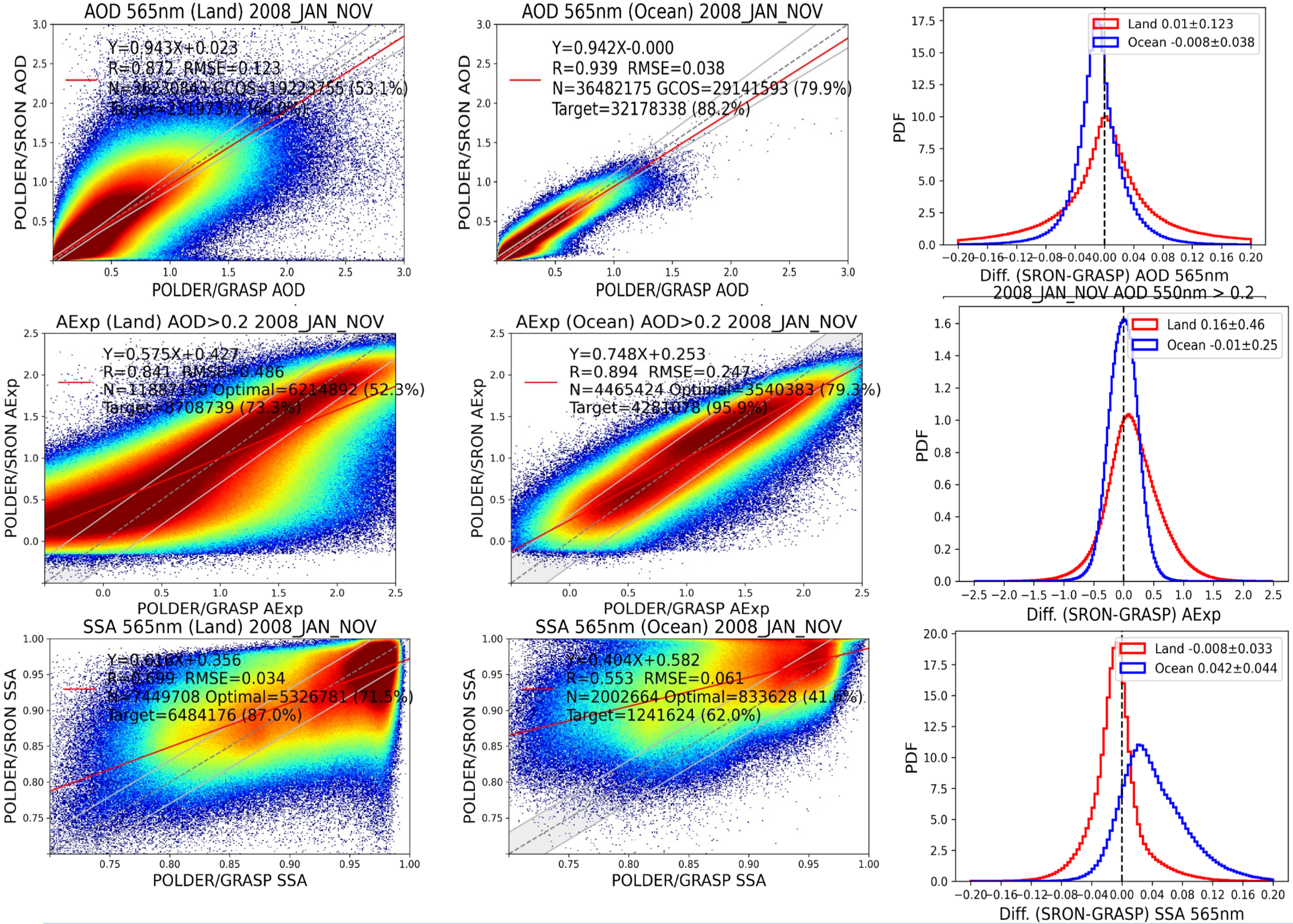

Figures by
Cheng Chen

Summary

- Both RemoTAP-SRON and GRASP improved significantly during the HARPOL and show good agreement with AERONET:
  - For AOD: similar performance of both.
  - For absorption (SSA): SRON-RemoTAP slightly better
  - For size (Angstrom Exponent): GRASP slightly better

- Overall, global comparison looks very good for AOD and reasonable for Angstrom Exponent and SSA.

- Regional difference occur of desert (AE) and biomass burning area (SSA, AOD)

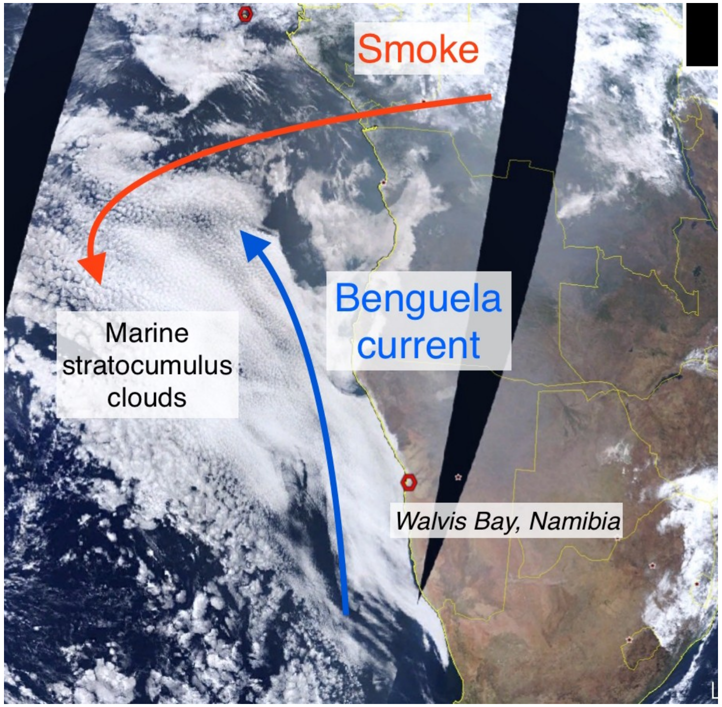

Aerosol SW absorption & direct radiative forcing over SEA in CMIP6 simulations.

Marc Mallet, Pierre Nabat, Martine Michou, Ben Johnson, Jim Haywood, Cheng Chen, Oleg Dubovik

The Southeast Atlantic: role of absorbing aerosols

- Smoke absorbing properties & surface albedo are crucial to quantify the sign of the forcing at TOA

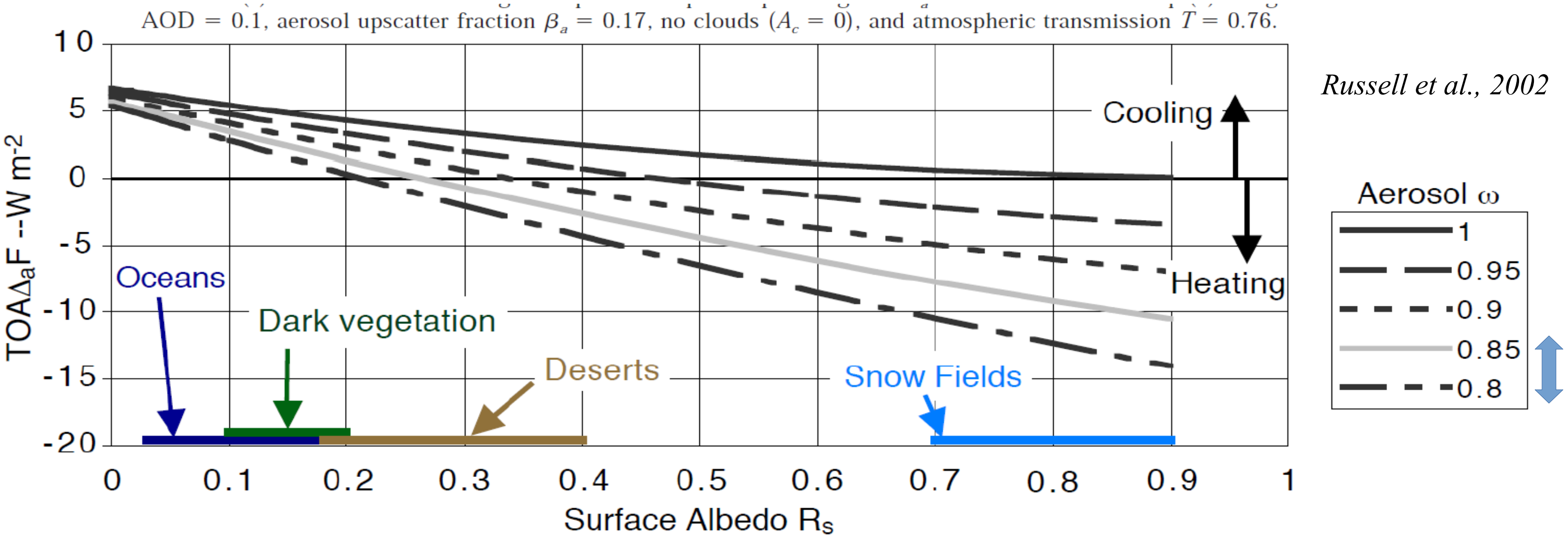

Russell et al., 2002

- BBA are <u>highly absorbing</u> over SEA

Zuidema et al. (2018) - LASIC
Pistone et al. (2019) - ORACLES
Wu et al. (2020) - CLARIFY
Chauvigné et al. (2021) - AEROCLOsA
Denjean et al. (2020) - DACCIWA

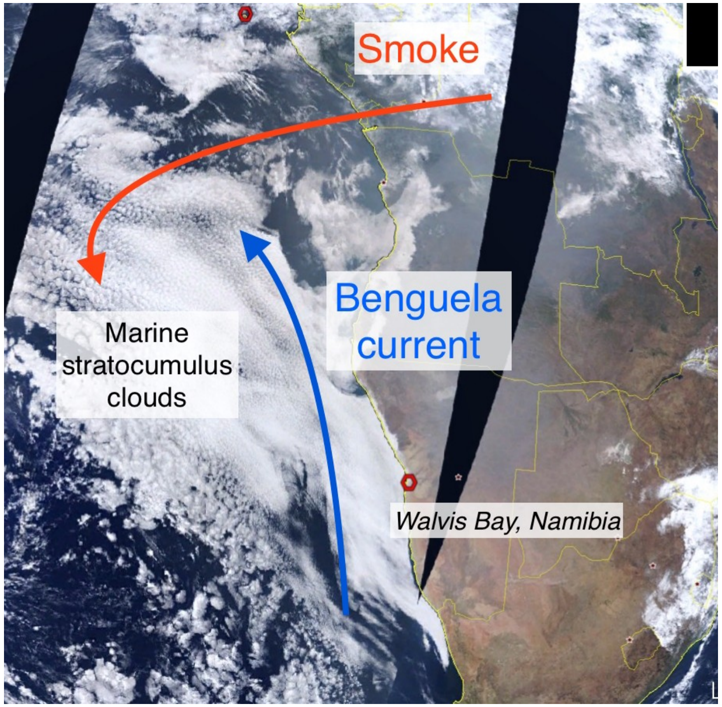

- Climate models struggle to simulate <u>low level Sc clouds</u> → impact on ocean surface albedo

- BBA are known to produce a positive direct effect over SEA

M. de Graaf et al., 2014
N. Feng, et al., 2015
M. S. Kacenelenbogen et al., 2019

The Southeast Atlantic: role of absorbing aerosols

- Objectives :
  - Do CMIP6 models correctly represent the optical properties of BBA ?
  - Do they simulate positive direct radiative forcing (TOA), solar absorption and additional radiative heating ?
- Evaluation using recent measurements (satellites / AERONET) and reanalysis

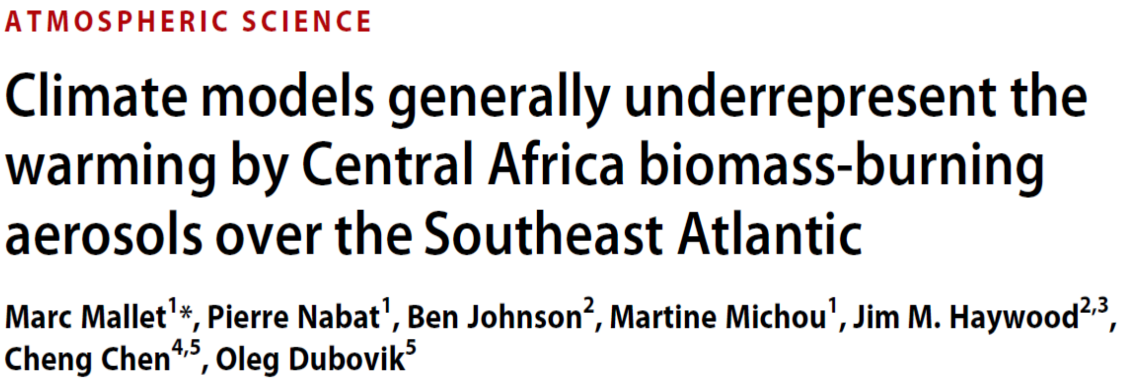

ATMOSPHERIC SCIENCE

Climate models generally underrepresent the warming by Central Africa biomass-burning aerosols over the Southeast Atlantic

Marc Mallet[1]*, Pierre Nabat[1], Ben Johnson[2], Martine Michou[1], Jim M. Haywood[2,3], Cheng Chen[4,5], Oleg Dubovik[5]

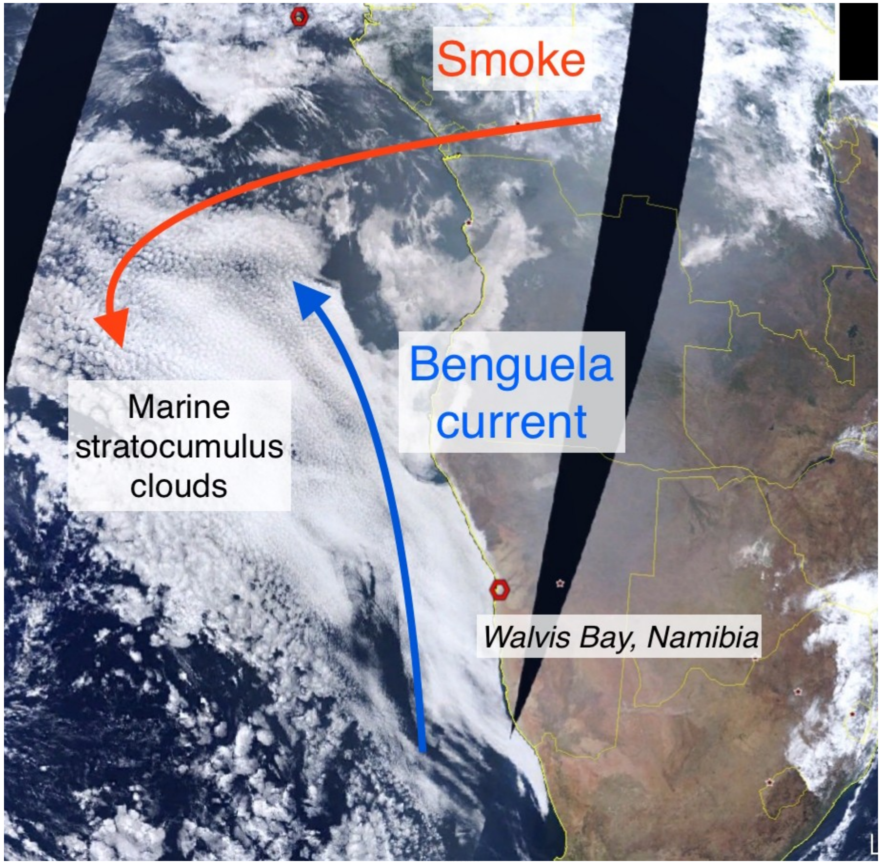

Do CMIP6 models correctly represent the optical properties of BBA ?

- SSA / 3 groups of models : correct (C), scattering (S), absorbing (A)

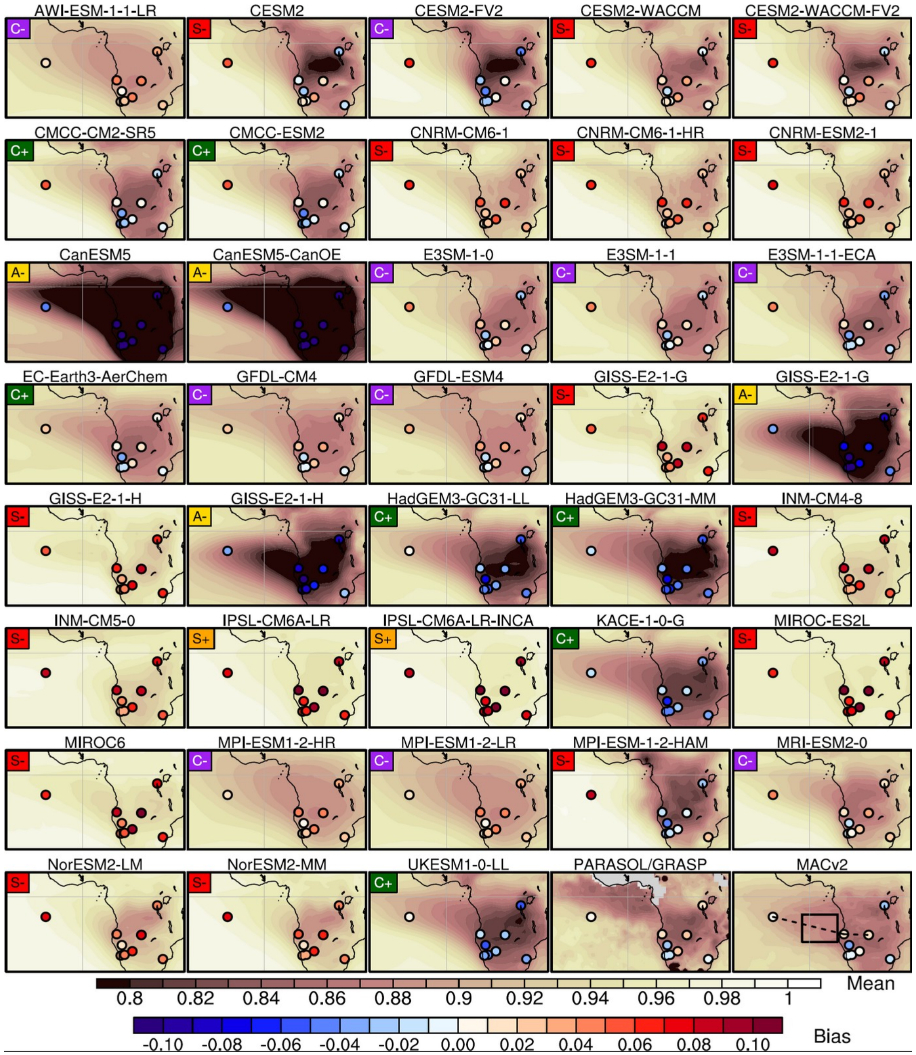

=> consistent seasonal cycle of SSA

=> low bias over land, <u>increasing over ocean</u>

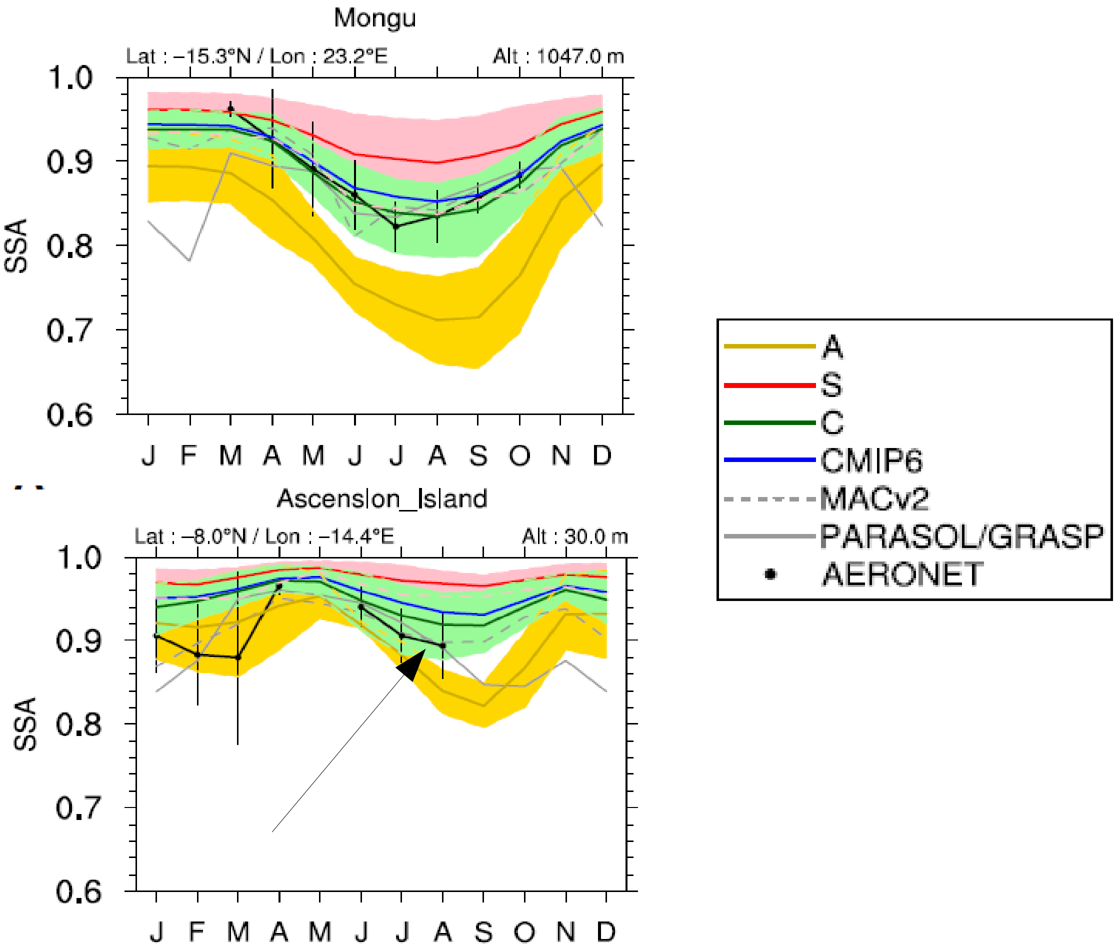

Do CMIP6 models correctly represent the optical properties of BBA ?

- SSA / 3 groups of models : correct (C), scattering (S), absorbing (A)

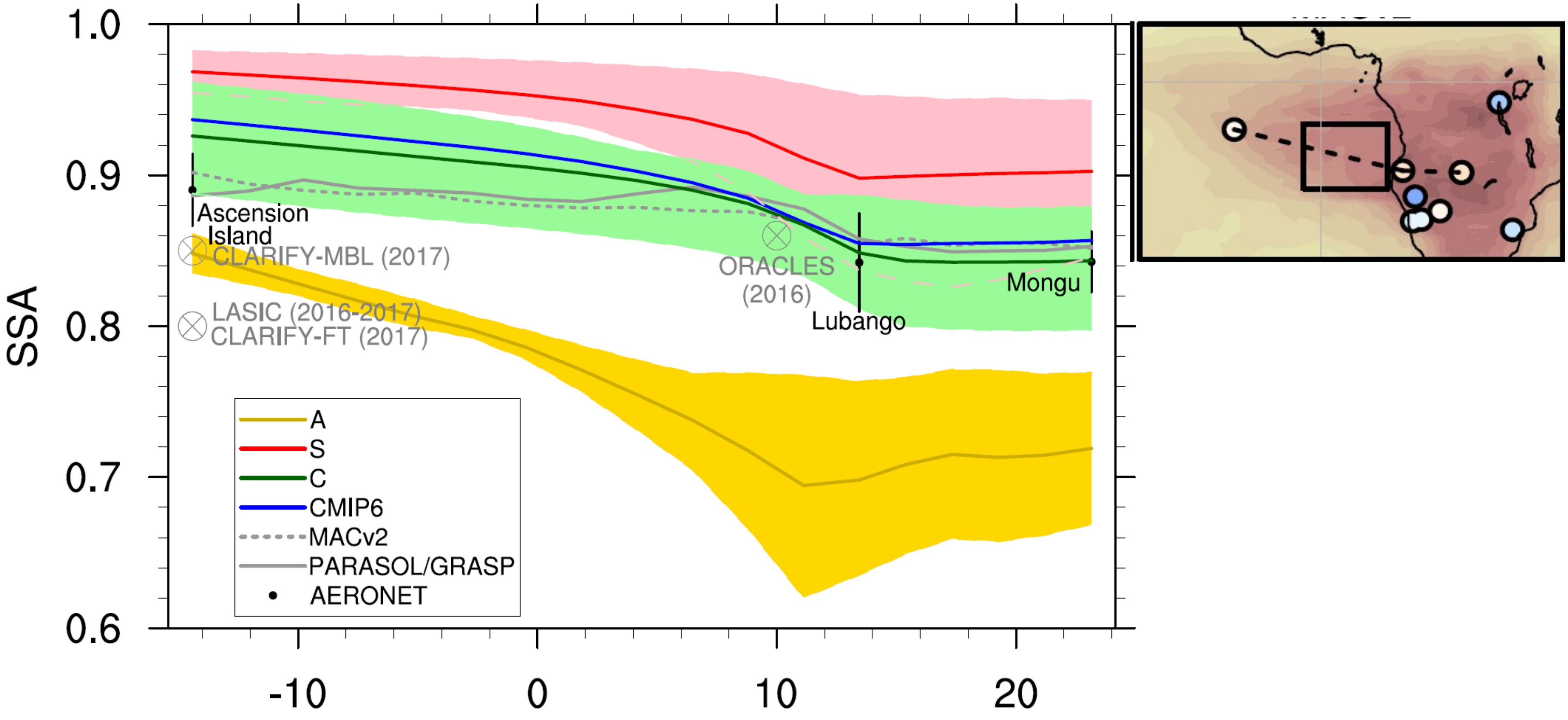

=> low bias over land, increasing over ocean

=> underestimation of SSA during the transport

Do CMIP6 models correctly represent the direct radiative forcing at TOA ?

Cloud fraction (CMIP6 historical, 1995-2014, bias from CALIPSO)
Classification for low cloud fraction: correct (+), underestimation (-)

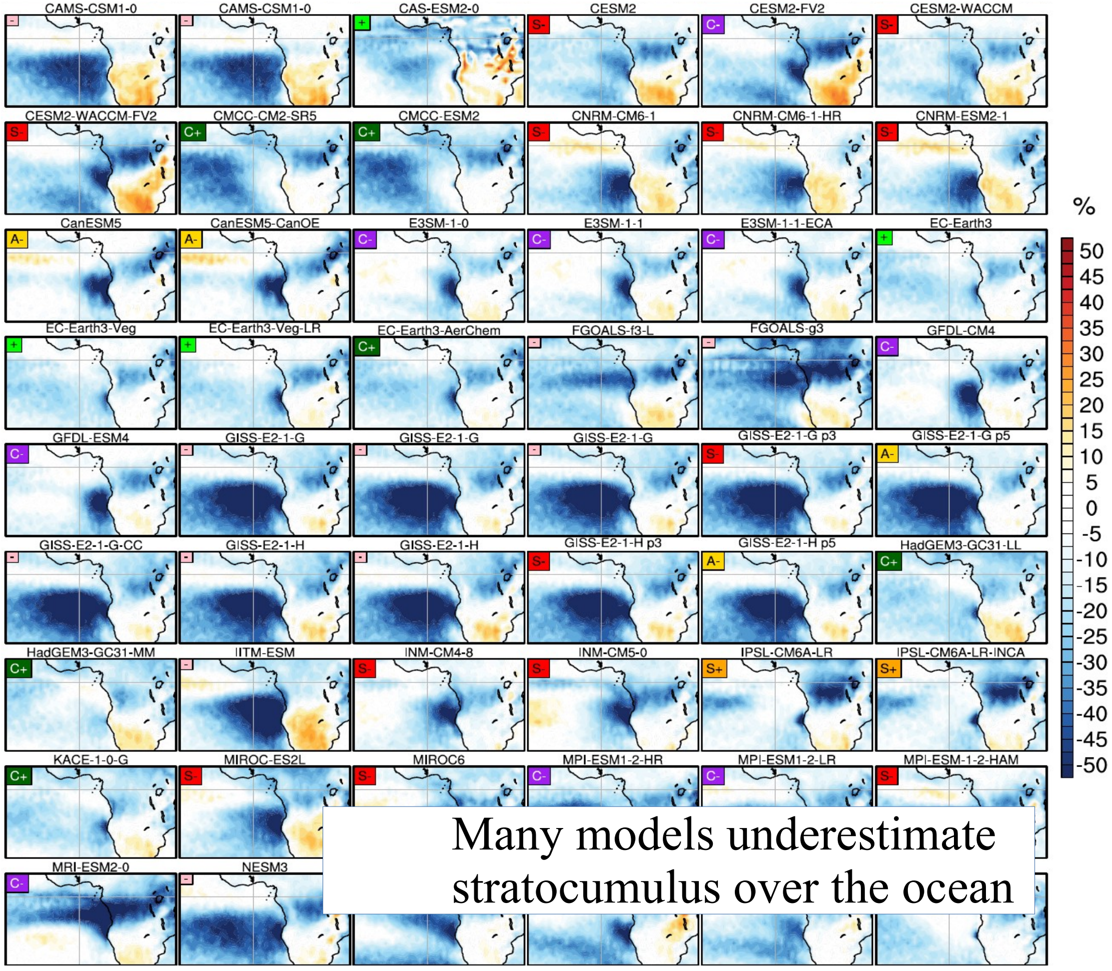

Many models underestimate stratocumulus over the ocean

Direct radiative forcing (SW) at TOA

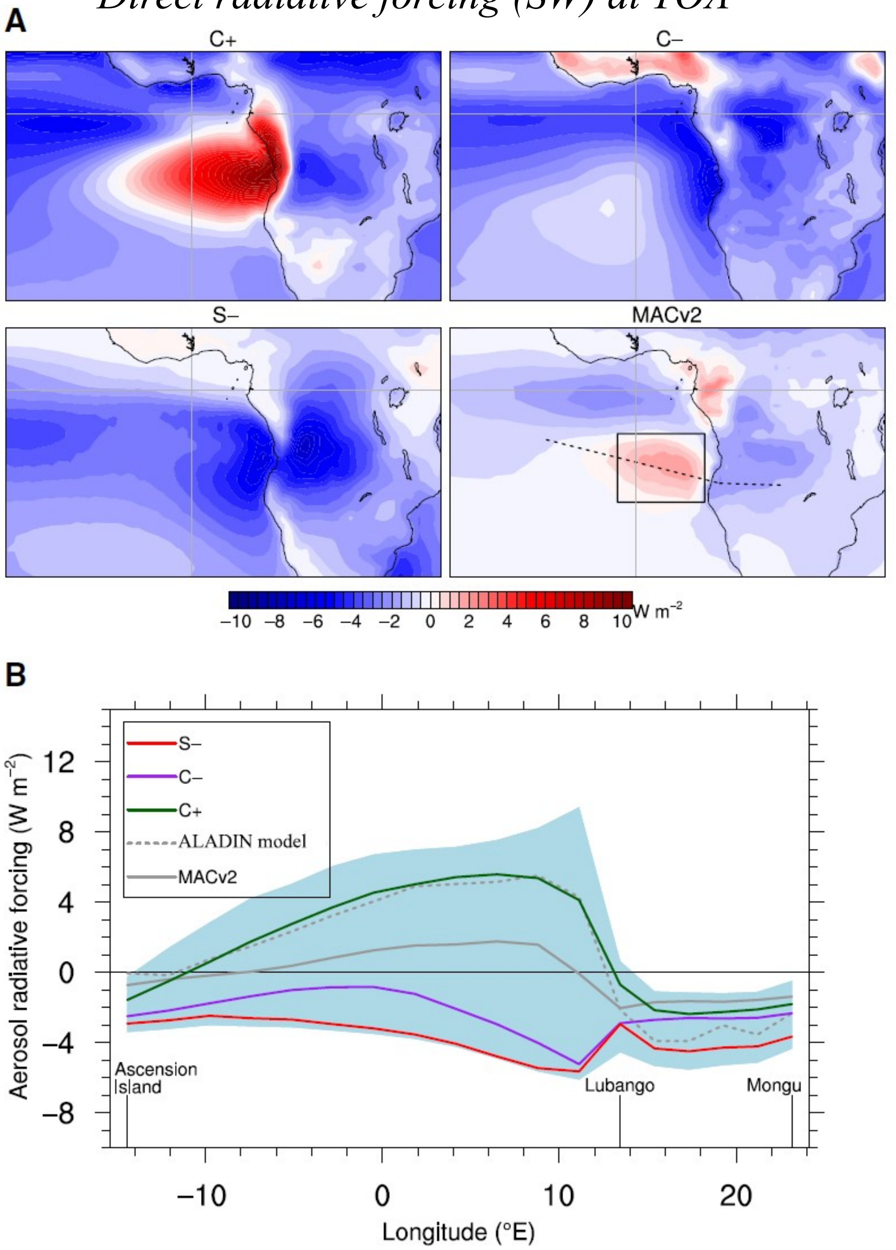

Summary : Aerosol SW absorption underestimated in Atlantic **+ lack of low clouds over ocean :**
→ negative bias in aerosol radiative forcing over SEA

Only C+ models (SSA + cloud cover correct, ~25 % of CMIP6 models) reproduce the positive forcing at TOA

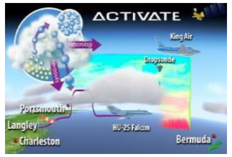

Aerosol Humidification Observed by the Airborne High Spectral Resolution Lidar-2

Richard Ferrare[1], John Hair[1], Chris Hostetler[1], David Harper[1], Shane Seaman[1], Taylor Shingler[1], Ewan Crosbie[2], Edward Winstead[2], Luke Ziemba[1], Michael Shook[1], Lee Thornhill[2], Marta Fenn[2], Marian Clayton[2], Amy Jo Scarino[2], Sharon Burton[1], Anthony Cook[1], Glenn Diskin[1], Rich Moore[1], Claire Robinson[2], Josh DiGangi[1], John Nowak[1], Armin Sorooshian[3], Sue van den Heever[4], Allison Collow[5,6], Arlindo da Silva[6], Bastiaan van Diedenhoven[7]

[1]NASA Langley Research Center, [2]SSAI/NASA/LaRC, [3]University of Arizona, [4]Colorado State University,
[5]Univ. of Maryland Baltimore County, [6]NASA Goddard Space Flight Center, [7]SRON

Data used in this study are from these missions:

1) NASA CAMP2Ex (Aug-Oct 2019) (Philippines)

- CAMP2Ex addresses aerosol and cloud microphysics
- NASA LaRC HSRL-2 deployed on P-3B aircraft for nadir viewing measurements
- P-3B, based at Clark Air Base, conducted 19 science flights between Aug. 24 and Oct. 5, 2019
- Dropsondes deployed from P-3B aircraft

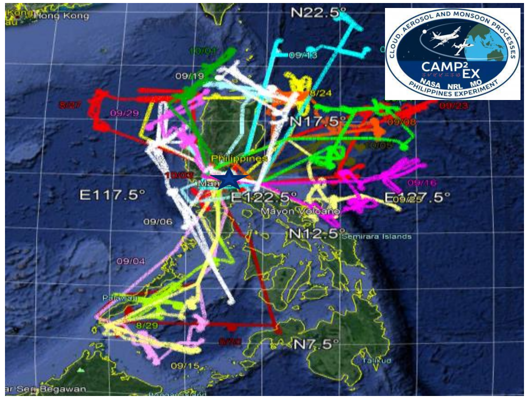

2) NASA EVS-3 ACTIVATE (Feb-Mar, Aug-Sep 2020; Jan-Jun, Dec 2021; Jan-Jun 2022; data used here are from 2020-2021)

- Focus on marine boundary layer (MBL) clouds off the US Mid-Atlantic Coast
- NASA LaRC HSRL-2 deployed on LaRC King Air aircraft for nadir viewing measurements, Dropsondes deployed from LaRC King Air aircraft
- In situ instruments deployed on NASA LaRC HU-25 Falcon aircraft to simultaneously measure BL clouds and aerosols below King Air

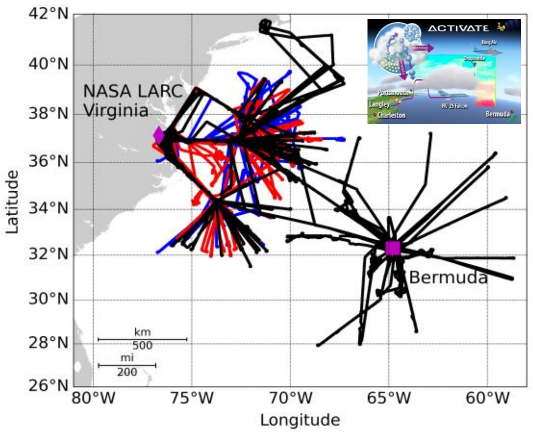

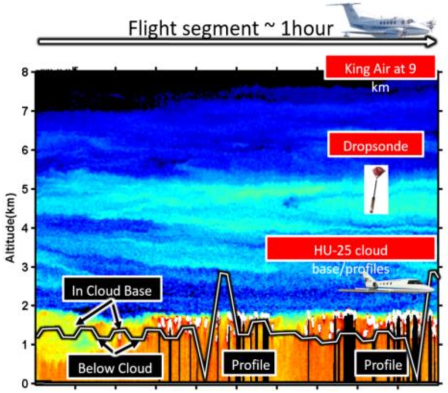

HSRL-2 Products from CAMP2Ex and ACTIVATE

- Aerosol Backscatter and Depolarization Profiles (355, 532, 1064 nm)
- Aerosol Extinction, Lidar Ratio, and AOT Profiles (355 and 532 nm)
- Aerosol Color Ratio Profiles (1064/532, 532/355)
- Aerosol Type
- Mixed Layer Heights
- Aerosol humidification enhancement factors for aerosols within well-mixed PBL are computed using HSRL-2 measurements of aerosol backscatter and dropsonde measurements of RH

HSRL-2 Aerosol Measurements show Variability with Relative Humidity

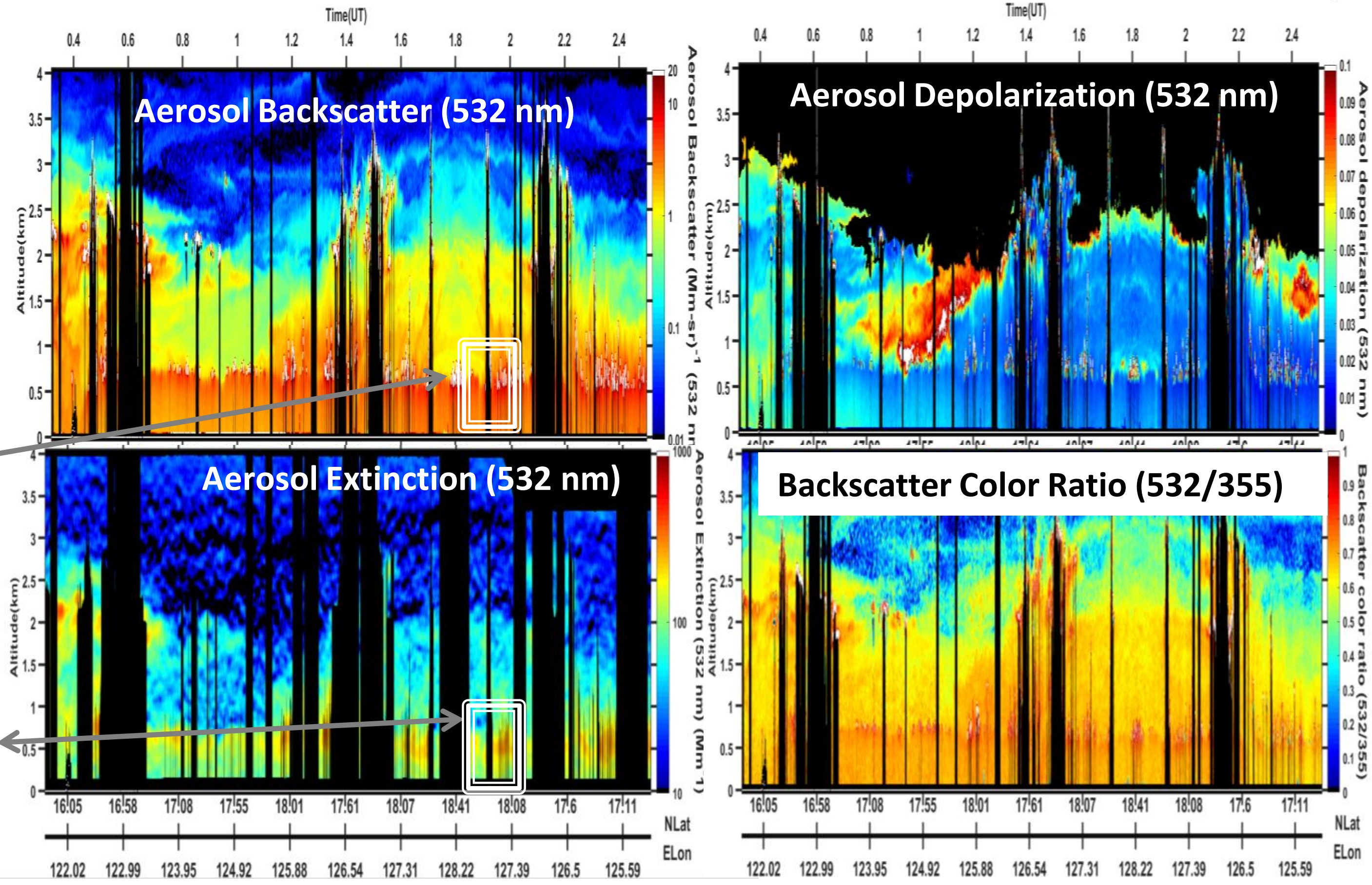

Expanded View of Aerosol Backscatter and Extinction Images

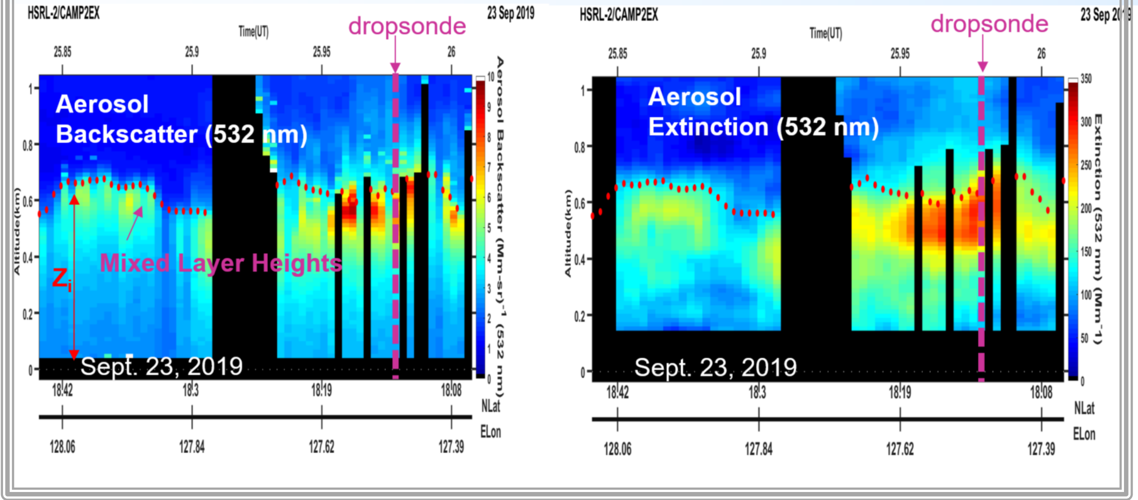

HSRL-2 data from CAMP2Ex at
https://www-air.larc.nasa.gov/cgi-bin/ArcView/camp2ex#HOSTETLER.CHRIS/
HSRL-2 data from ACTIVATE at
https://www-air.larc.nasa.gov/cgi-bin/ArcView/activate.2019#HOSTETLER.CHRIS/

Quantifying the Aerosol Enhancement Factors Associated with the Increase in Relative Humidity (RH) using HSRL-2 and Dropsondes

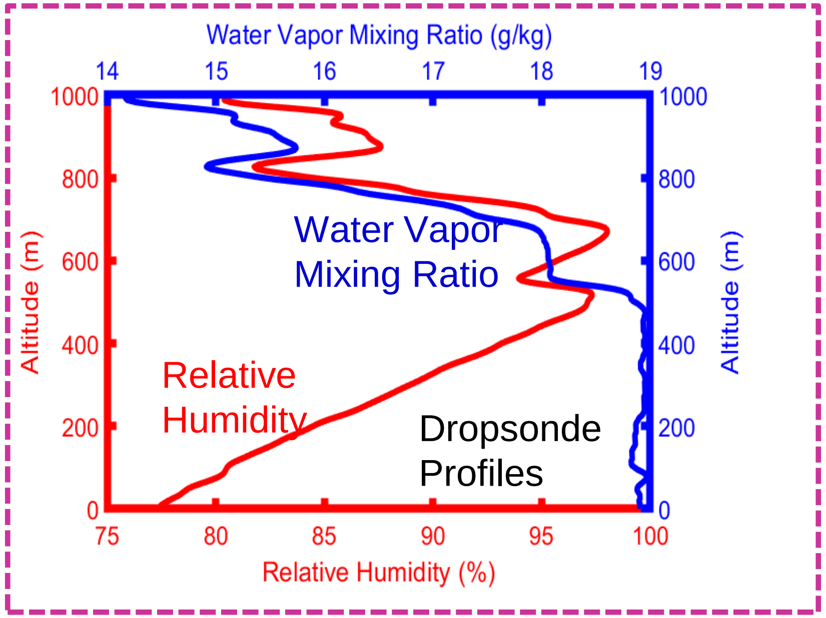

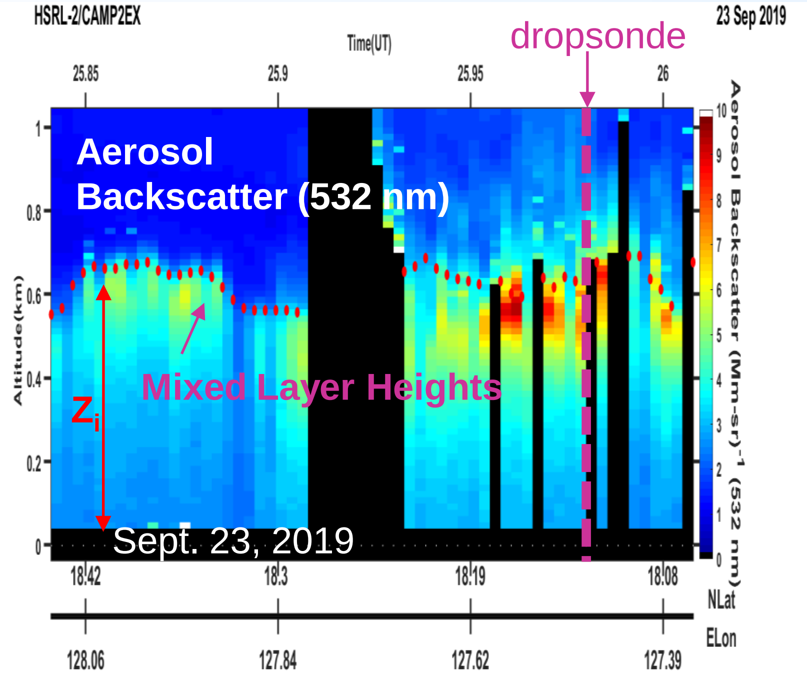

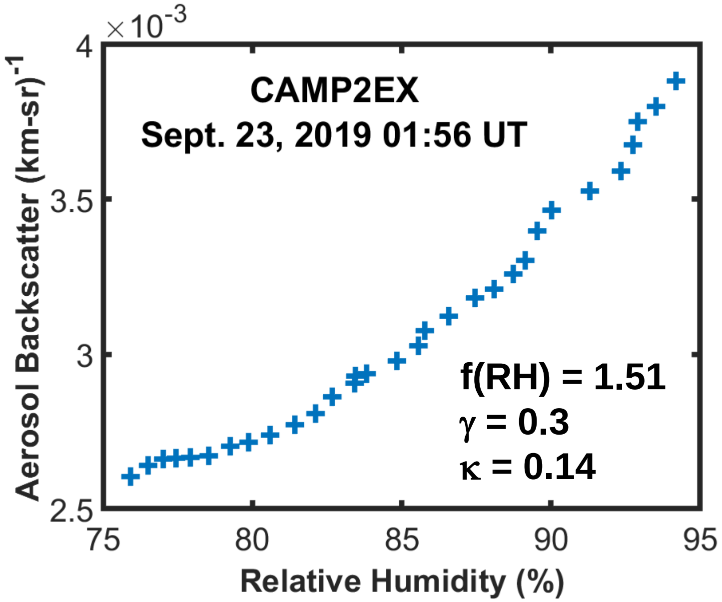

- As RH increases with height within Mixed Layer, hygroscopic particles take on water, so aerosol backscatter and extinction increase.
- To quantify this increase, we compute aerosol enhancement factor f(RH), gamma (γ), kappa (κ) within the mixed layer (i.e. Z/Z_i <1)
- Aerosol backscatter profiles from HSRL2; RH profiles from dropsondes
- Mixed Layer Height (Z_i) derived from HSRL-2 aerosol backscatter profiles
- Restrict cases to nearly constant water vapor mixing ratio so aerosol properties vary with RH and not due to changes in concentration
- Values in the comparisons are for f(RH=80%/RH=20%)

$$f(RH) = \frac{\beta(RH)}{\beta(RH_o)} = [\frac{(100-RH_o)}{(100-RH)}]^{\gamma}$$

$$\cong 1 + \kappa_{bsc}[\frac{RH}{100-RH}]$$

- f(RH), gamma (γ), kappa (κ) (HSRL-2) for aerosol backscatter and extinction are similar

Aerosol Humidification Factors derived from HSRL-2/dropsondes are typically larger than from airborne in situ measurements

- Average f(RH=80%/RH=20%) (532 nm) derived from HSRL-2 and dropsonde data was about 1.68 during both CAMP2Ex and ACTIVATE
- This value was higher than the corresponding values from airborne in situ measurements

- Higher f(RH) values derived from HSRL-2 & dropsonde data are likely because lidar observes both fine and coarse (sea salt) aerosol in contrast to in situ measurements of only fine mode aerosol
- Example from CAMP2Ex Sept. 21, 2019 flight
  - In situ f(RH) ~ 1.0-1.1
  - HSRL-2/dropsonde f(RH) ~ 1.5

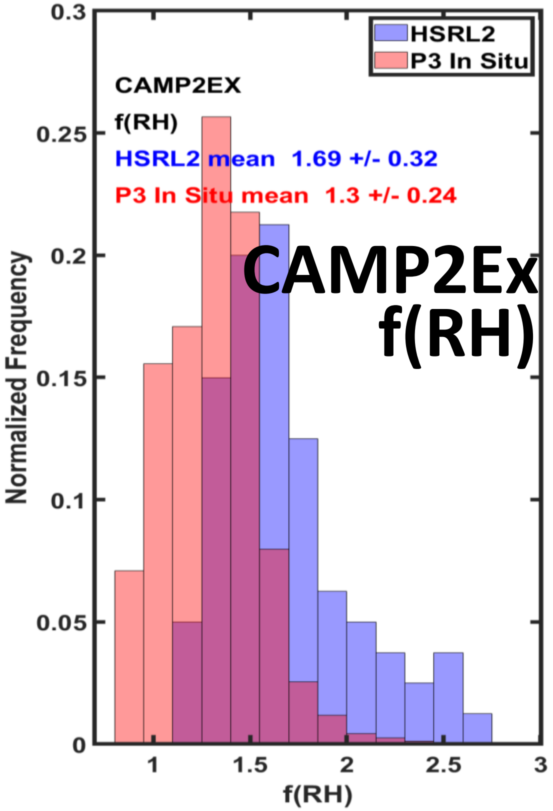

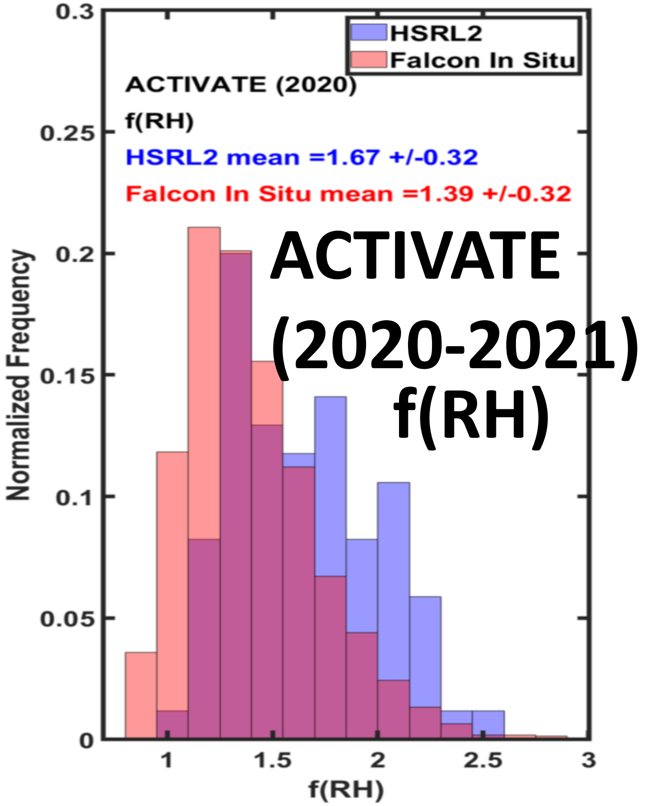

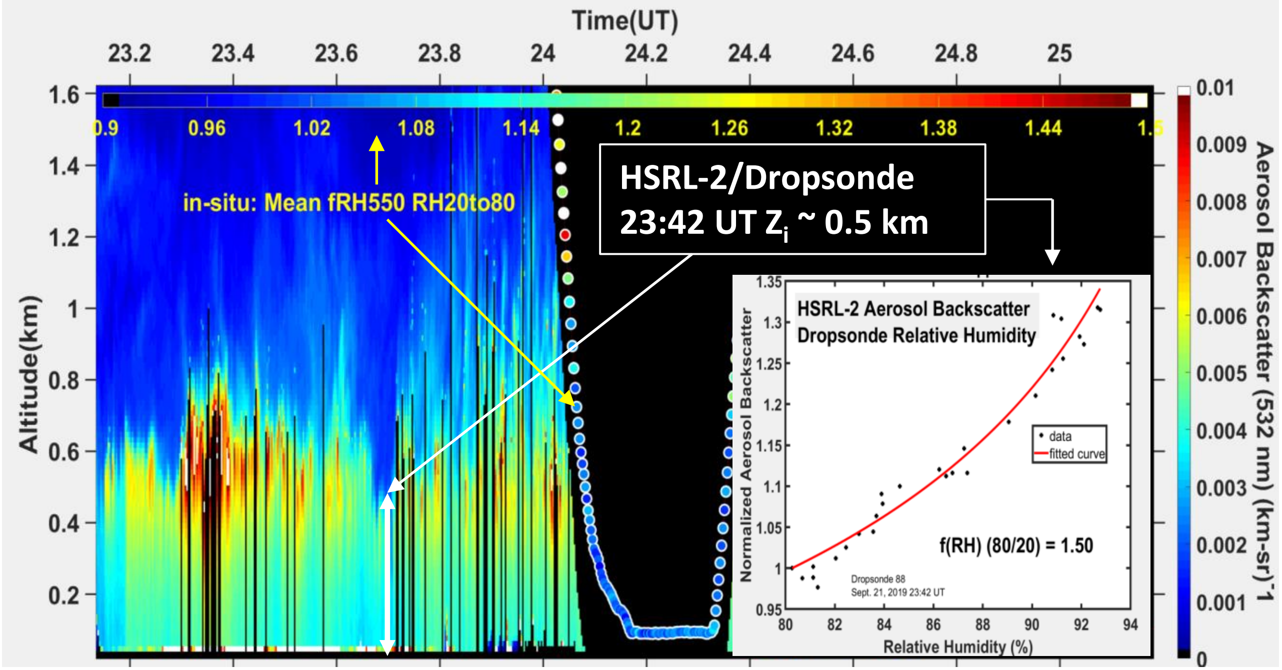

Comparison of f(RH) derived from HSRL-2/dropsonde measurements with GEOS model and associated with aerosol type

- GEOS model values of f(RH) are higher and have less variability than those derived from both HSRL-2&dropsonde and airborne in situ values

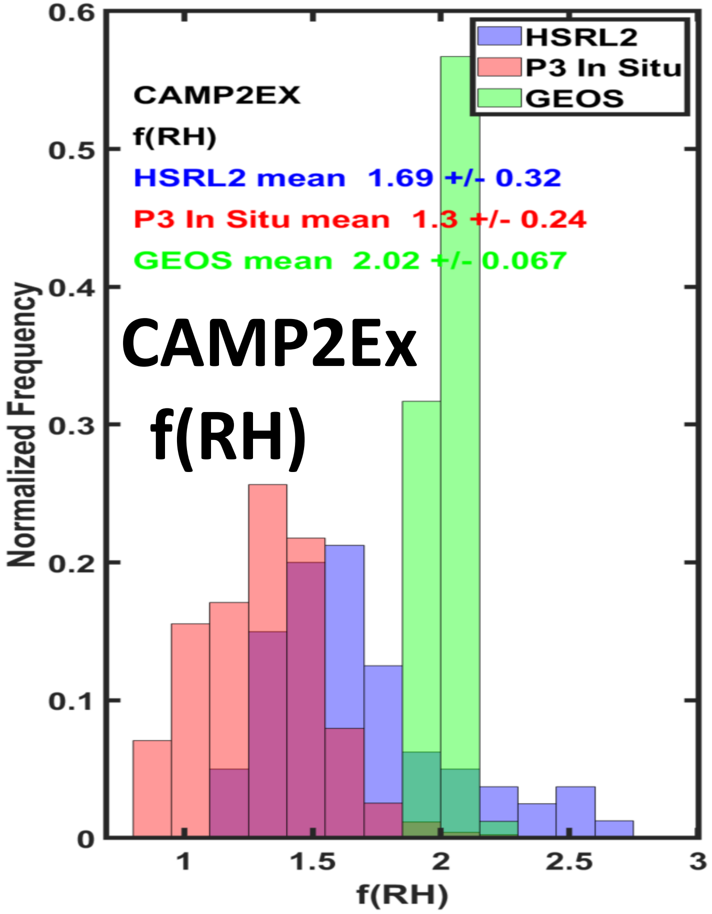

- HSRL-2/dropsonde f(RH) appear most consistent with marine & urban aerosol

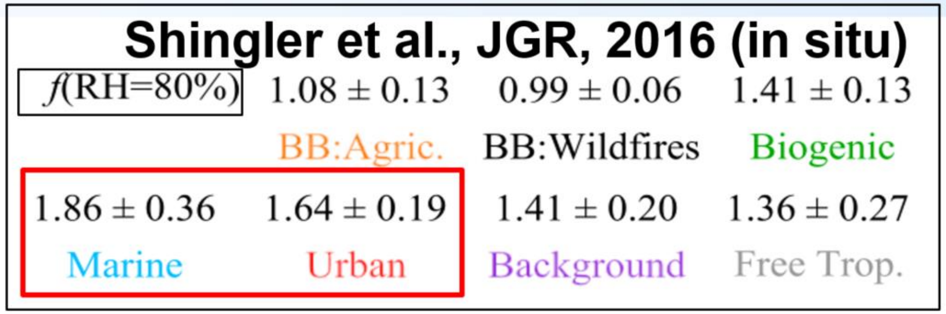

Shingler et al., JGR, 2016 (in situ)

f(RH=80%)	1.08 ± 0.13	0.99 ± 0.06	1.41 ± 0.13
	BB:Agric.	BB:Wildfires	Biogenic
1.86 ± 0.36	1.64 ± 0.19	1.41 ± 0.20	1.36 ± 0.27
Marine	Urban	Background	Free Trop.

- During CAMP2Ex, f(RH) values derived from HSRL-2/dropsonde data were somewhat higher for urban and lower for biomass burning

CAMP2Ex HSRL-2 + dropsonde f(RH) vs. HSRL aerosol type

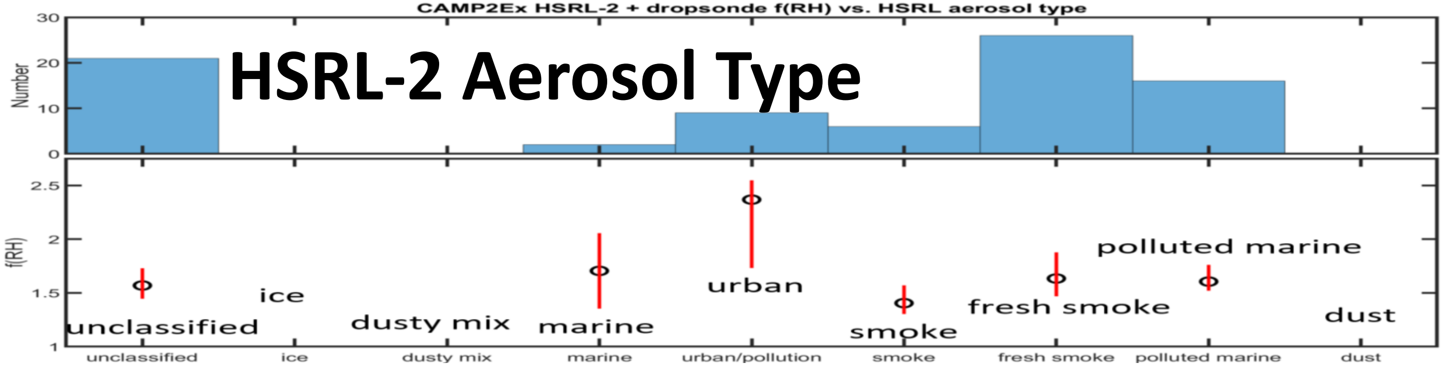

CAMP2Ex HSRL-2 + dropsonde f(RH) vs. Chemical Influence Regime

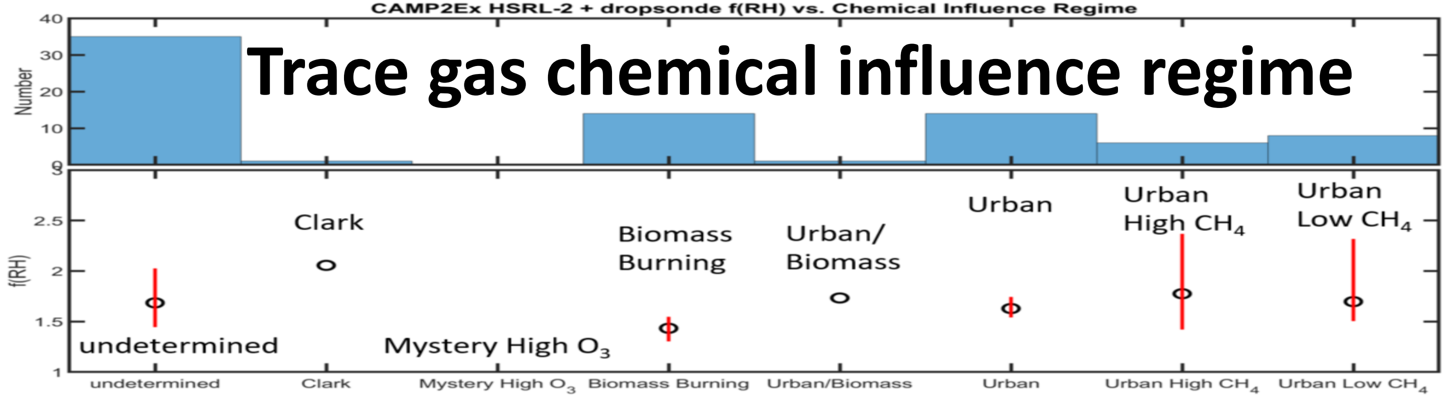

A comprehensive analysis of dynamic error estimates provided by GRASP algorithm for satellite observations

Milagros E. Herrera Oleg Dubovik Benjamin Torres Tatsiana Lapyonak David Fuertes Cheng Chen
Anton Lopatin Pavel Litvinov Christian Matar

GRASP SAS, Remote Sensing Developments, Lezennes, France
Laboratoire d'Optique Atmosphérique, CNRS – Université Lille , France

Basic concepts of formal propagation techniques

Example: Dynamic error estimates in GRASP

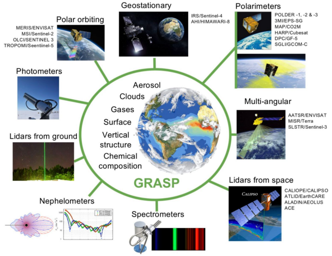

$$\hat{\mathbf{a}}_{estim} - \mathbf{a}_{real} = \Delta\hat{\mathbf{a}}_{ran} + \Delta\hat{\mathbf{a}}_{sys}$$

$$\underbrace{< \Delta\hat{\mathbf{a}}_{ran} >= 0}_{\textbf{random}} \qquad \underbrace{< \Delta\hat{\mathbf{a}}_{sys} >\neq 0}_{\textbf{systematic-bias}}$$

Dubovik et al., 2021

$$\boxed{\mathbf{C}_{\hat{\mathbf{a}}} = \left\langle (\Delta\hat{\mathbf{a}}_{ran} + \Delta\hat{\mathbf{a}}_{sys})(\Delta\hat{\mathbf{a}}_{ran} + \Delta\hat{\mathbf{a}}_{sys})^T \right\rangle = \mathbf{C}_{\Delta\hat{\mathbf{a}}_{ran}} + (\hat{\mathbf{a}}_{bias})(\hat{\mathbf{a}}_{bias})^T}$$

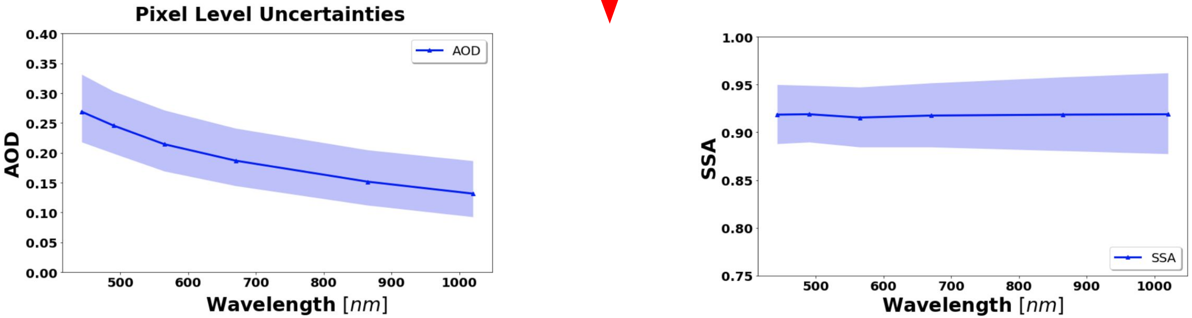

Concept of dynamic error estimates in GRASP

- Based on rigorous statistical estimation approach
- A priori information is included using Multi-Term LSM (Least Square Method)
- Bias and input error variance estimated using **miss-fit of observations**

e.g. *Dubovik et al., 2021*

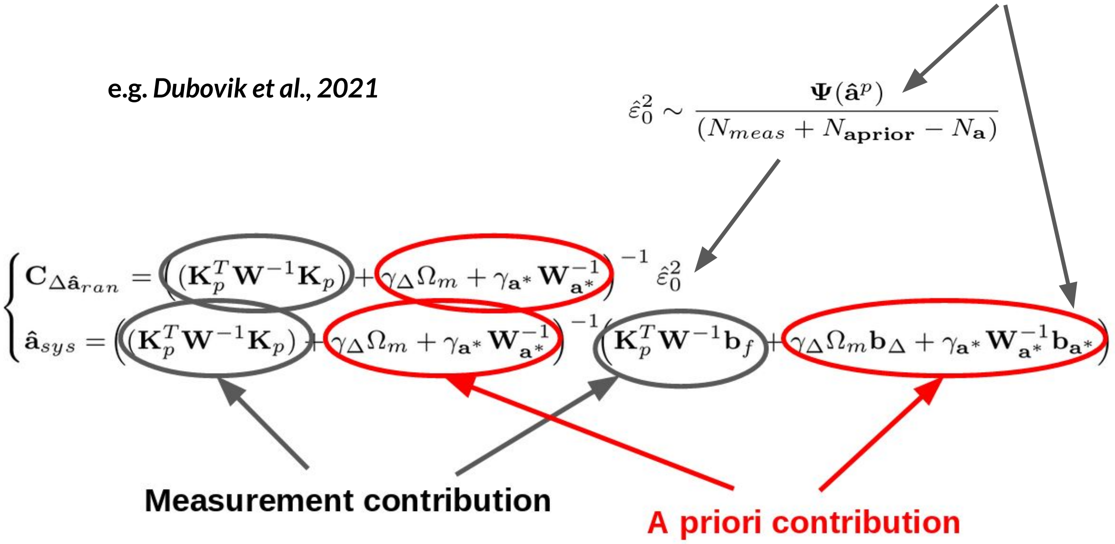

$$\hat{\varepsilon}_0^2 \sim \frac{\mathbf{\Psi}(\hat{\mathbf{a}}^p)}{(N_{meas} + N_{\mathbf{aprior}} - N_{\mathbf{a}})}$$

$$\begin{cases} \mathbf{C}_{\Delta\hat{\mathbf{a}}_{ran}} = \left((\mathbf{K}_p^T\mathbf{W}^{-1}\mathbf{K}_p) + \gamma_\Delta\Omega_m + \gamma_{\mathbf{a}^*}\mathbf{W}_{\mathbf{a}^*}^{-1}\right)^{-1} \hat{\varepsilon}_0^2 \\ \hat{\mathbf{a}}_{sys} = \left((\mathbf{K}_p^T\mathbf{W}^{-1}\mathbf{K}_p) + \gamma_\Delta\Omega_m + \gamma_{\mathbf{a}^*}\mathbf{W}_{\mathbf{a}^*}^{-1}\right)^{-1}\left(\mathbf{K}_p^T\mathbf{W}^{-1}\mathbf{b}_f + \gamma_\Delta\Omega_m\mathbf{b}_\Delta + \gamma_{\mathbf{a}^*}\mathbf{W}_{\mathbf{a}^*}^{-1}\mathbf{b}_{\mathbf{a}^*}\right) \end{cases}$$

Measurement contribution

A priori contribution

Error estimates = Diagonal elements of covariance matrix

Error variances

$$Cov(\mathbf{a}) = \begin{pmatrix} \sigma_1^2 & \sigma_1\sigma_2\rho_{12} & \sigma_1\sigma_3\rho_{13} & \cdots \\ \sigma_2\sigma_1\rho_{21} & \sigma_2^2 & \sigma_2\sigma_3\rho_{23} & \cdots \\ \sigma_3\sigma_1\rho_{31} & \sigma_3\sigma_2\rho_{32} & \sigma_3^2 & \cdots \\ \vdots & \vdots & \vdots & \ddots \end{pmatrix}$$

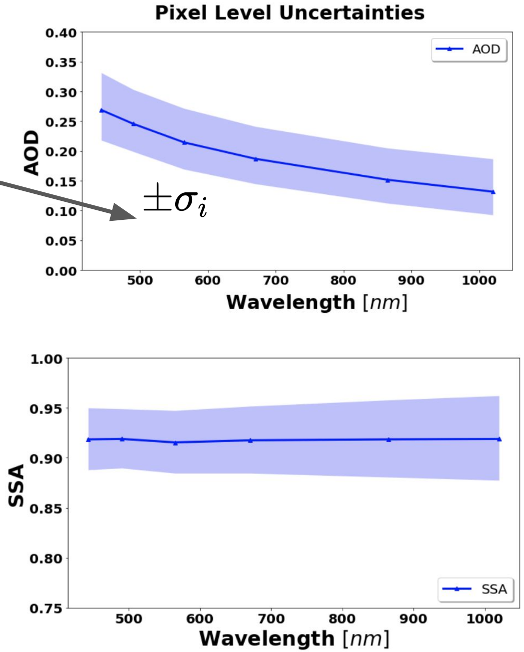

Example for POLDER/PARASOL-like retrievals

  - ○ **bias and random noise: +3% in I and +0.01 in Q and U.**

Initial approach

$$\sigma_{tot} = \sqrt{\sigma_{ran}^2 + \sigma_{bias}^2}$$

$$\sigma_{bias}^2 = \sigma_{lm}^2 + \sigma_{misfit}^2$$

- Bias and input error variance estimated using **miss-fit of observations**

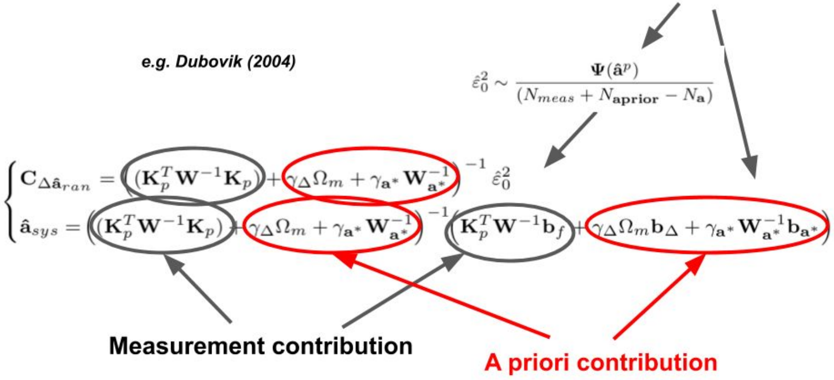

e.g. Dubovik (2004)

$$\hat{\varepsilon}_0^2 \sim \frac{\Psi(\hat{\mathbf{a}}^p)}{(N_{meas}+N_{\mathbf{aprior}}-N_{\mathbf{a}})}$$

$$\begin{cases} \mathbf{C}_{\Delta\hat{\mathbf{a}}_{ran}} = \left((\mathbf{K}_p^T\mathbf{W}^{-1}\mathbf{K}_p)+(\gamma_\Delta\Omega_m+\gamma_{\mathbf{a}^*}\mathbf{W}_{\mathbf{a}^*}^{-1})\right)^{-1}\hat{\varepsilon}_0^2 \\ \hat{\mathbf{a}}_{sys} = \left((\mathbf{K}_p^T\mathbf{W}^{-1}\mathbf{K}_p)+(\gamma_\Delta\Omega_m+\gamma_{\mathbf{a}^*}\mathbf{W}_{\mathbf{a}^*}^{-1})\right)^{-1}\left((\mathbf{K}_p^T\mathbf{W}^{-1}\mathbf{b}_f)+(\gamma_\Delta\Omega_m\mathbf{b}_\Delta+\gamma_{\mathbf{a}^*}\mathbf{W}_{\mathbf{a}^*}^{-1}\mathbf{b}_{\mathbf{a}^*})\right) \end{cases}$$

Measurement contribution

A priori contribution

Problem: Not all the bias can be seen in the miss-fit of observation

Mongu

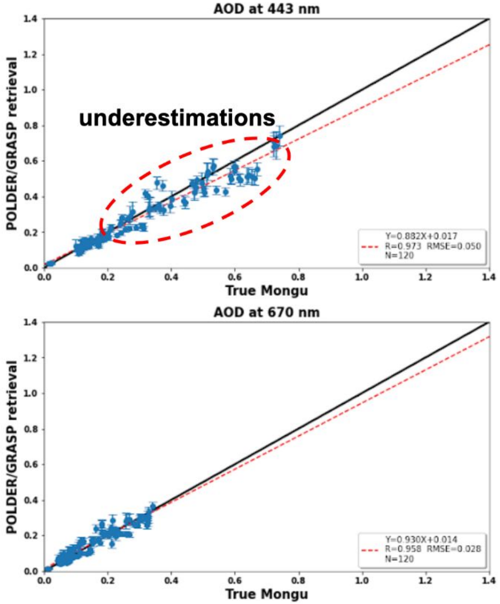

Dubovik et al., 2021

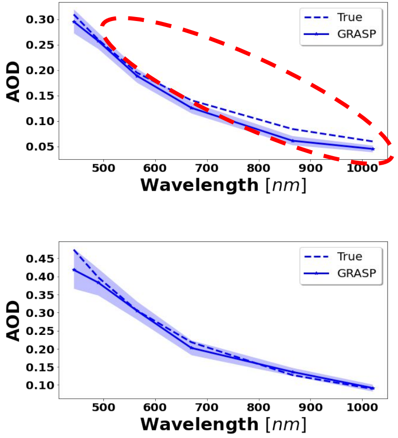

Example for POLDER/PARASOL-like retrievals

- ○ **bias and random noise: +3% in I and +0.01 in Q and U.**

Improved approach

$$\sigma_{tot} = \sqrt{\sigma_{ran}^2 + \sigma_{bias}^2}$$

$$\sigma_{bias}^2 = \sigma_{lm}^2 + \sigma_{misfit}^2 + \frac{1}{N}\sum_{k=1}^{N}\sigma_k^2$$

Proposed solution:

- We consider to include potential bias in the equation for systematic component

$$\hat{\mathbf{a}}_{bias}^{\pm} \approx \left(\mathbf{K}_p^T\mathbf{W}^{-1}\mathbf{K}_p\right)^{-1}\left(\mathbf{K}_p^T\mathbf{W}^{-1}(\mathbf{b}_f \pm \mathbf{b}_{bias})\right)$$

we assume three bias: **positive, negative and zero-bias.**

Mongu

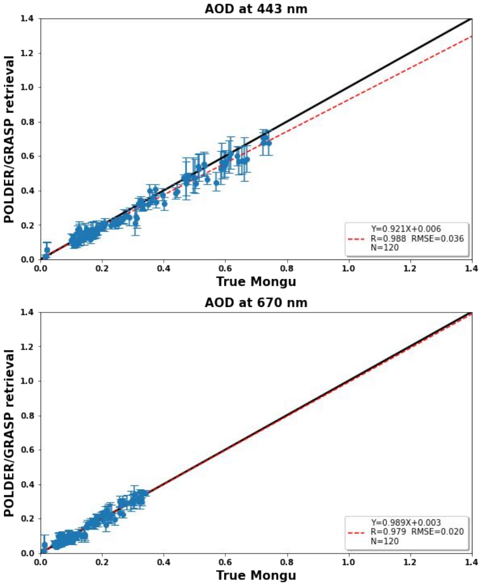

Pixel level:

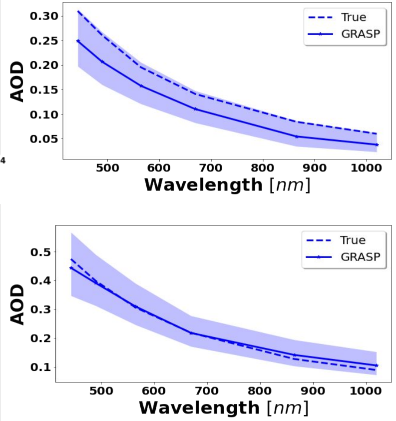

Real applications:

- Example for POLDER/PARASOL retrievals over Mongu

Improved approach

$$\sigma_{tot} = \sqrt{\sigma_{ran}^2 + \sigma_{bias}^2}$$

$$\sigma_{bias}^2 = \sigma_{lm}^2 + \sigma_{misfit}^2 + \frac{1}{N}\sum_{k=1}^{N}\sigma_k^2$$

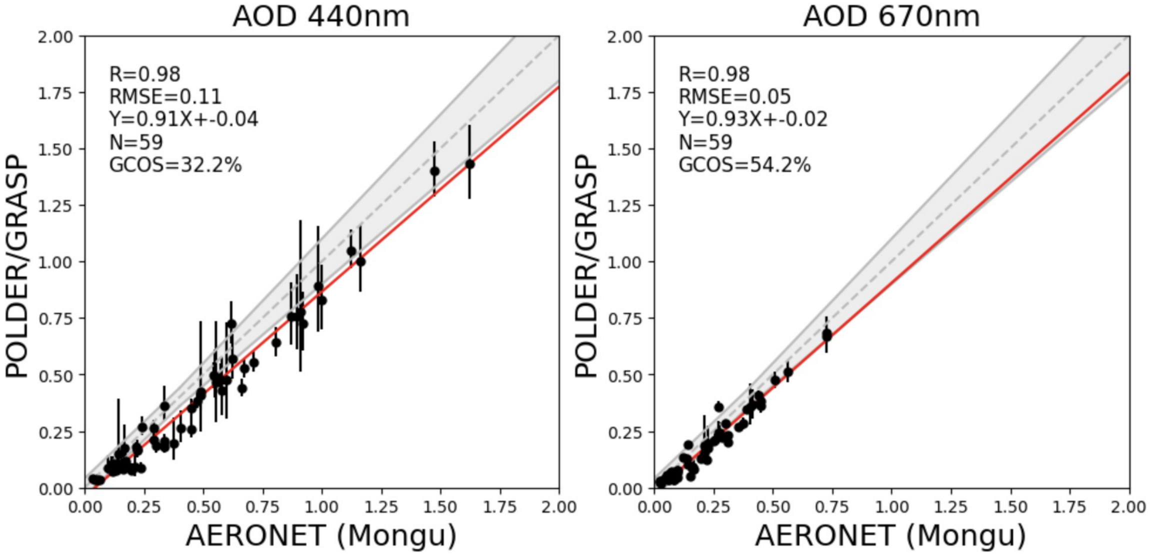

Analysis of Non-diagonal elements of covariance matrix:

$$Cov(\mathbf{a}) = \begin{pmatrix} \sigma_1^2 & \sigma_1\sigma_2\rho_{12} & \sigma_1\sigma_3\rho_{13} & \cdots \\ \sigma_2\sigma_1\rho_{21} & \sigma_2^2 & \sigma_2\sigma_3\rho_{23} & \cdots \\ \sigma_3\sigma_1\rho_{31} & \sigma_3\sigma_2\rho_{32} & \sigma_3^2 & \cdots \\ \vdots & \vdots & \vdots & \ddots \end{pmatrix}$$

Correlation matrix

$$Corr(\mathbf{a}) = \begin{pmatrix} 1 & \rho_{12} & \rho_{13} & \cdots \\ \rho_{21} & 1 & \rho_{23} & \cdots \\ \rho_{31} & \rho_{32} & 1 & \cdots \\ \vdots & \vdots & \vdots & \ddots \end{pmatrix}$$

Some more details

Correlation matrix:

- Example for POLDER/PARASOL-like retrievals

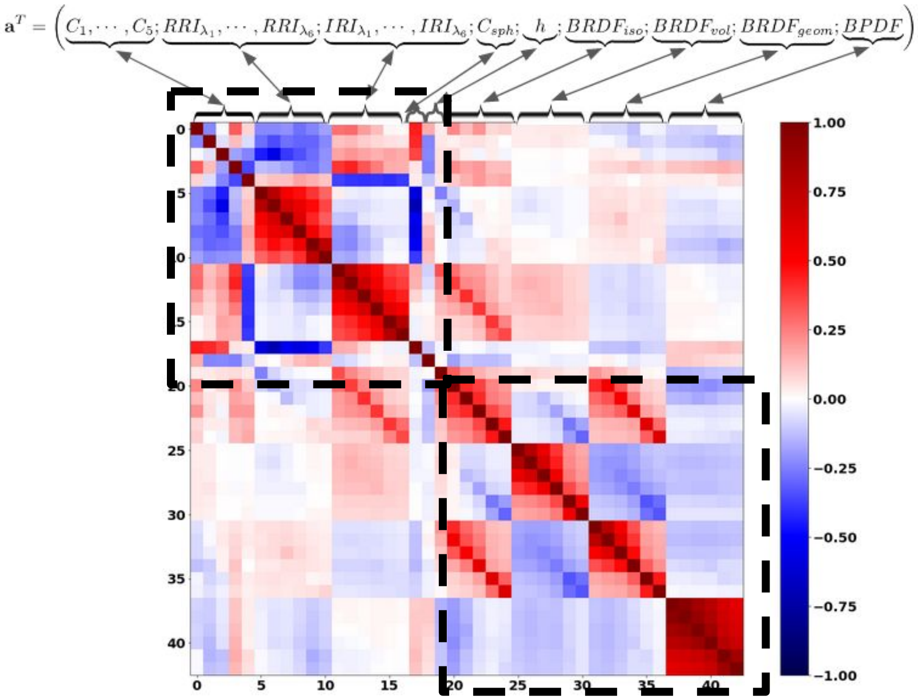

$$\mathbf{a}^T = \left(\underbrace{C_1,\cdots,C_5};\underbrace{RRI_{\lambda_1},\cdots,RRI_{\lambda_6}};\underbrace{IRI_{\lambda_1},\cdots,IRI_{\lambda_6}};\underbrace{C_{sph}};\underbrace{h};\underbrace{BRDF_{iso}};\underbrace{BRDF_{vol}};\underbrace{BRDF_{geom}};\underbrace{BPDF}\right)$$

Summary

- **GRASP** provides rigorous estimates of dynamic retrieval errors;
- Diagonal elements of covariance matrix are being used for validation of **GRASP** error estimates for many applications;
- Improvements modeling systematic errors (bias) in **GRASP** algorithm have been shown;
- **GRASP** generates the full covariance matrices that provide interesting inside for understanding retrieval tendencies.

Thank you!